

## Review

# Localization of Functional Activity in the Central Nervous System by Measurement of Glucose Utilization with Radioactive Deoxyglucose

Louis Sokoloff

*Laboratory of Cerebral Metabolism, National Institute of Mental Health, U.S. Public Health Service, Department of Health and Human Services, Bethesda, Maryland*

The brain is a complex, heterogeneous organ composed of many anatomical and functional components with markedly different levels of functional activity that vary independently with time and function. Other tissues are generally far more homogeneous, with most of their cells functioning similarly and synchronously in response to a common stimulus or regulatory influence. The central nervous system, however, consists of innumerable subunits, each integrated into its own set of functional pathways and networks and subserving only one or a few of the many activities in which the nervous system participates. Understanding how the nervous system functions requires a knowledge not only of the mechanisms of excitation and inhibition, but even more so of their precise localization in the nervous system and the relationships of neural subunits to specific functions.

Historically, studies of the central nervous system have concentrated heavily on localization of function and mapping of pathways related to specific functions. These have been carried out neuroanatomically and histologically with staining and degeneration techniques, behaviorally with ablation and stimulation techniques, electrophysiologically with electrical recording and evoked electrical responses, and histochemically with a variety of techniques, including fluorescent and

immunofluorescent methods and autoradiography of orthograde and retrograde axoplasmic flow. Many of these conventional methods suffer from a sampling problem. They generally permit examination of only one potential pathway at a time, and only positive results are interpretable. Furthermore, the demonstration of a pathway reveals only a potential for function; it does not reveal its significance in normal function.

Tissues that do physical and/or chemical work—such as heart, kidney, and skeletal muscle—exhibit a close relationship between energy metabolism and the level of functional activity. The existence of a similar relationship in the tissues of the central nervous system has been more difficult to prove, partly because of uncertainty about the nature of the work associated with nervous functional activity, but mainly because of the difficulty in assessing the levels of functional and metabolic activities in the same functional component of the brain at the same time. Much of our present knowledge of cerebral energy metabolism *in vivo* has been obtained by means of the nitrous oxide technique of Kety and Schmidt (1948a) and its modifications (Scheinberg and Stead, 1949; Lassen and Munck, 1955; Eklöf et al., 1973; Gjedde et al., 1975), which measure the average rates of energy metabolism in the brain as a whole. These methods have demonstrated changes in cerebral metabolic rate in association with gross or diffuse alterations of cerebral function and/or structure, as, for example, those that occur during postnatal development, aging, senility, anesthesia, disorders of consciousness, and convulsive states (Kety, 1950, 1957; Lassen, 1959; Sokoloff, 1960,

---

Address correspondence and reprint requests to Dr. Sokoloff at Laboratory of Cerebral Metabolism, National Institute of Mental Health, Bldg. 36, Rm. 1A-27, 9000 Rockville Pike, Bethesda, Maryland 20205.

*Abbreviations used:* DG, 2-deoxyglucose; DG-6-P, 2-deoxyglucose-6-phosphate; 6-G-P, glucose-6-phosphate.

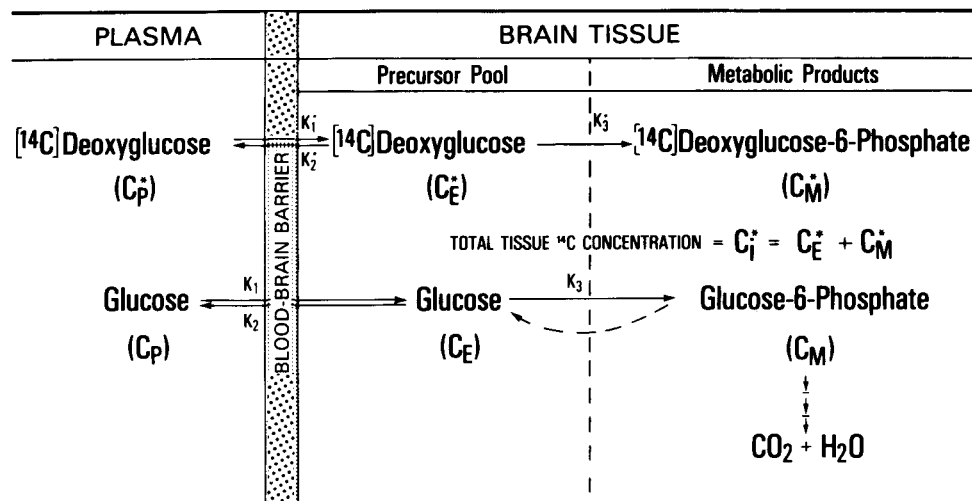


**FIG. 1. A:** Diagrammatic representation of the theoretical model.  $C_i^*$  represents the total  $^{14}\text{C}$  concentration in a single homogeneous tissue of the brain.  $C_p^*$  and  $C_p$  represent the concentrations of  $[^{14}\text{C}]$ deoxyglucose ( $[^{14}\text{C}]$ DG) and glucose in the arterial plasma, respectively;  $C_E^*$  and  $C_E$  represent their respective concentrations in the tissue pools that serve as substrates for hexokinase.  $C_M^*$  represents the concentration of  $[^{14}\text{C}]$ deoxyglucose-6-phosphate in the tissue. The constants  $k_1^*$ ,  $k_2^*$ , and  $k_3^*$ , represent the rate constants for carrier-mediated transport of  $[^{14}\text{C}]$ DG from plasma to tissue, for carrier-mediated transport back from tissue to plasma, and for phosphorylation by hexokinase, respectively. The constants  $k_1$ ,  $k_2$ , and  $k_3$  are the equivalent rate constants for glucose.  $[^{14}\text{C}]$ DG and glucose share and compete for the carrier that transports both between plasma and tissue and for hexokinase which phosphorylates them to their respective hexose-6-phosphates. The dashed arrow represents the possibility of glucose-6-phosphate hydrolysis by glucose-6-phosphatase activity, if any. (From Sokoloff, et al. 1977; Sokoloff, 1978b.)

1976). They have not detected changes in cerebral metabolic rate in a number of conditions with, perhaps, more subtle alterations in cerebral functional activity, for example, deep slow-wave sleep, performance of mental arithmetic, sedation and tranquilization, schizophrenia, and LSD-induced psychosis (Kety, 1950; Lassen, 1959; Sokoloff, 1969). It is possible that there are no changes in cerebral energy metabolism in these conditions. The apparent lack of change could also be explained by either a redistribution of local levels of functional and metabolic activity without significant change in the average of the brain as a whole or the restriction of altered metabolic activity to regions too small to be detected in measurements of the brain as a whole. What has clearly been needed is a method that measures the rates of energy metabolism in specific discrete regions of the brain in normal and altered states of functional activity.

In pursuit of this goal, Kety and his associates (Landau et al., 1955; Freygang and Sokoloff, 1958; Kety, 1960; Reivich et al., 1969) developed a quantitative autoradiographic technique to measure the local tissue concentrations of chemically inert, diffusible, radioactive tracers, which they used to determine the rates of blood flow simultaneously in all

the structural components visible and identifiable in autoradiographs of serial sections of the brain. The application of this quantitative autoradiographic technique to the determination of local cerebral metabolic rate has proved to be more difficult because of the inherently greater complexity of the problem and the unsuitability of the labeled species of the normal substrates of cerebral energy metabolism, oxygen and glucose. The radioisotopes of oxygen have too short a physical half-life. Both oxygen and glucose are too rapidly converted to carbon dioxide, and  $\text{CO}_2$  is too rapidly cleared from the cerebral tissues. Sacks (1957), for example, has found in man significant losses of  $^{14}\text{CO}_2$  from the brain within 2 minutes after the onset of an intravenous infusion of  $[^{14}\text{C}]$ glucose, labeled either uniformly, in the C-1, C-2, or C-6 positions. These limitations of  $[^{14}\text{C}]$ glucose have been avoided by the use of 2-deoxy-D- $[^{14}\text{C}]$ glucose ( $[^{14}\text{C}]$ DG), a labeled analogue of glucose with special properties that make it particularly appropriate for this application (Sokoloff et al., 1977). It is metabolized through part of the pathway of glucose metabolism at a definable rate relative to that of glucose. Unlike glucose, however, its product,  $[^{14}\text{C}]$ deoxyglucose-6-phosphate ( $[^{14}\text{C}]$ DG-6-P), is essentially trapped in

General Equation for Measurement of Reaction Rates with Tracers:

$$\text{Rate of Reaction} = \frac{\text{Labeled Product Formed in Interval of Time, 0 to T}}{\left[ \begin{array}{c} \text{Isotope Effect} \\ \text{Correction Factor} \end{array} \right] \left[ \begin{array}{c} \text{Integrated Specific Activity} \\ \text{of Precursor} \end{array} \right]}$$

Operational Equation of [<sup>14</sup>C]Deoxyglucose Method:

$$R_i = \frac{\text{Labeled Product Formed in Interval of Time, 0 to T}}{\left[ \begin{array}{c} \text{Total } ^{14}\text{C in Tissue} \\ \text{at Time, T} \\ C_i^*(T) \end{array} \right] - \left[ \begin{array}{c} ^{14}\text{C in Precursor Remaining in Tissue at Time, T} \\ k_i^* e^{-(k_2^* + k_3^*)T} \int_0^T C_p^* e^{(k_2^* + k_3^*)t} dt \end{array} \right]}$$

$$R_i = \frac{\left[ \begin{array}{c} \lambda \cdot V_m^* \cdot K_m \\ \Phi \cdot V_m \cdot K_m^* \end{array} \right] \left[ \begin{array}{c} \int_0^T \left( \frac{C_p^*}{C_p} \right) dt \\ \text{Integrated Plasma} \\ \text{Specific Activity} \end{array} \right] - \left[ \begin{array}{c} e^{-(k_2^* + k_3^*)T} \int_0^T \left( \frac{C_p^*}{C_p} \right) e^{(k_2^* + k_3^*)t} dt \\ \text{Correction for Lag in Tissue} \\ \text{Equilibration with Plasma} \end{array} \right]}{\text{Integrated Precursor Specific Activity in Tissue}}$$

**FIG. 1. B:** Operational equation of radioactive deoxyglucose method and its functional anatomy. T represents the time at the termination of the experimental period; λ equals the ratio of the distribution space of deoxyglucose in the tissue to that of glucose; Φ equals the fraction of glucose which, once phosphorylated, continues down the glycolytic pathway; and  $K_m^*$  and  $V_m^*$  and  $K_m$  and  $V_m$  represent the familiar Michaelis-Menten kinetic constants of hexokinase for deoxyglucose and glucose, respectively. The other symbols are the same as those defined in Fig. 1A. (From Sokoloff, 1978b.)

the tissues, allowing the application of the quantitative autoradiographic technique. The use of radioactive DG to trace glucose utilization and the autoradiographic technique to achieve regional localization has recently led to the development of a method that measures the rates of glucose utilization simultaneously in all components of the central nervous system in the normal conscious state and during experimental physiological, pharmacological, and pathological conditions (Sokoloff et al., 1977). Because the procedure is so designed that the concentrations of radioactivity in the tissues during autoradiography are more or less proportional to the rates of glucose utilization, the autoradiographs provide pictorial representations of the relative rates of glucose utilization in all the cerebral structures visualized. Numerous studies with this method have established that there is a close relationship between functional activity and energy metabolism in the central nervous system (Plum et al., 1976; Sokoloff, 1977), and the method has become a potent new tool for mapping functional

neural pathways on the basis of evoked metabolic responses.

### Theory

The method is derived from a model based on the biochemical properties of DG (Fig. 1A) (Sokoloff et al., 1977). 2-Deoxyglucose is transported bidirectionally between blood and brain by the same carrier that transports glucose across the blood-brain barrier (Bidder, 1968; Bachelard, 1971; Oldendorf, 1971). In the cerebral tissues it is phosphorylated by hexokinase to DG-6-P (Sols and Crane, 1954). Deoxyglucose and glucose are, therefore, competitive substrates for both blood-brain transport and hexokinase-catalyzed phosphorylation. Unlike glucose-6-phosphate (G-6-P), however, which is metabolized further, eventually to CO<sub>2</sub> and water and to a lesser degree via the hexosemonophosphate shunt, DG-6-P cannot be converted to fructose-6-phosphate and is not a substrate for G-6-P dehydrogenase (Sols and Crane,

1954). There is very little glucose-6-phosphatase activity in brain (Hers, 1957) and even less deoxyglucose-6-phosphatase activity (Sokoloff et al., 1977). Deoxyglucose-6-phosphate, once formed, is therefore essentially trapped in the cerebral tissues, at least long enough for the duration of the measurement.

If the interval of time is kept short enough, for example, less than 1 hour, to allow the assumption of negligible loss of [ $^{14}\text{C}$ ]DG-6-P from the tissues, then the quantity of [ $^{14}\text{C}$ ]DG-6-P accumulated in any cerebral tissue at any given time following the introduction of [ $^{14}\text{C}$ ]DG into the circulation is equal to the integral of the rate of [ $^{14}\text{C}$ ]DG phosphorylation by hexokinase in that tissue during that interval of time. This integral is in turn related to the amount of glucose that has been phosphorylated over the same interval, depending on the time courses of the relative concentrations of [ $^{14}\text{C}$ ]DG and glucose in the precursor pools and the Michaelis-Menten kinetic constants for hexokinase with respect to both [ $^{14}\text{C}$ ]DG and glucose. With cerebral glucose consumption in a steady state, the

amount of glucose phosphorylated during the interval of time equals the steady-state flux of glucose through the hexokinase-catalyzed step multiplied by the duration of the interval, and the net rate of flux of glucose through this step equals the rate of glucose utilization.

These relationships can be mathematically defined and an operational equation derived if the following assumptions are made: (1) a steady state for glucose (i.e., constant plasma glucose concentration and constant rate of glucose consumption) throughout the period of the procedure; (2) homogeneous tissue compartment within which the concentrations of [ $^{14}\text{C}$ ]DG and glucose are uniform and exchange directly with the plasma; and (3) that [ $^{14}\text{C}$ ]DG is present in tracer concentrations (i.e., molecular concentrations of free [ $^{14}\text{C}$ ]DG essentially equal to zero). The operational equation which defines  $R_i$ , the rate of glucose consumption per unit mass of tissue,  $i$ , in terms of measurable variables is presented in Fig. 1B.

The rate constants are determined in a separate group of animals by a nonlinear, iterative process

TABLE 1. Values of rate constants in the normal conscious albino rat

Structure	Rate constants (min <sup>-1</sup> )			Distribution volume (ml/g) $k_1^*/(k_2^* + k_3^*)$	Half-life of precursor pool (min) $\log 2/(k_2^* + k_3^*)$
	$k_1^*$	$k_2^*$	$k_3^*$		
<u>Gray Matter</u>					
Visual cortex	0.189 ± 0.048	0.279 ± 0.176	0.063 ± 0.040	0.553	2.03
Auditory cortex	0.226 ± 0.068	0.241 ± 0.198	0.067 ± 0.057	0.734	2.25
Parietal cortex	0.194 ± 0.051	0.257 ± 0.175	0.062 ± 0.045	0.608	2.17
Sensorimotor cortex	0.193 ± 0.037	0.208 ± 0.112	0.049 ± 0.035	0.751	2.70
Thalamus	0.188 ± 0.045	0.218 ± 0.144	0.053 ± 0.043	0.694	2.56
Medial geniculate body	0.219 ± 0.055	0.259 ± 0.164	0.055 ± 0.040	0.697	2.21
Lateral geniculate body	0.172 ± 0.038	0.220 ± 0.134	0.055 ± 0.040	0.625	2.52
Hypothalamus	0.158 ± 0.032	0.226 ± 0.119	0.043 ± 0.032	0.587	2.58
Hippocampus	0.169 ± 0.043	0.260 ± 0.166	0.056 ± 0.040	0.535	2.19
Amygdala	0.149 ± 0.028	0.235 ± 0.109	0.032 ± 0.026	0.558	2.60
Caudate-putamen	0.176 ± 0.041	0.200 ± 0.140	0.061 ± 0.050	0.674	2.66
Superior colliculus	0.198 ± 0.054	0.240 ± 0.166	0.046 ± 0.042	0.692	2.42
Pontine gray matter	0.170 ± 0.040	0.246 ± 0.142	0.037 ± 0.033	0.601	2.45
Cerebellar cortex	0.225 ± 0.066	0.392 ± 0.229	0.059 ± 0.031	0.499	1.54
Cerebellar nucleus	0.207 ± 0.042	0.194 ± 0.111	0.038 ± 0.035	0.892	2.99
Mean ± SEM	0.189 ± 0.012	0.245 ± 0.040	0.052 ± 0.010	0.647 ± 0.073	2.39 ± 0.40
<u>White Matter</u>					
Corpus callosum	0.085 ± 0.015	0.135 ± 0.075	0.019 ± 0.033	0.552	4.50
Genu of corpus callosum	0.076 ± 0.013	0.131 ± 0.075	0.019 ± 0.034	0.507	4.62
Internal capsule	0.077 ± 0.015	0.134 ± 0.085	0.023 ± 0.039	0.490	4.41
Mean ± SEM	0.079 ± 0.008	0.133 ± 0.046	0.020 ± 0.020	0.516 ± 0.171	4.51 ± 0.90

From Sokoloff et al., 1977.

which provides the least-squares best-fit of an equation which defines the time course of total tissue  $^{14}\text{C}$  concentration in terms of the time, the history of the plasma concentration, and the rate constants to the experimentally determined time courses of tissue and plasma concentrations of  $^{14}\text{C}$  (Sokoloff et al., 1977). The rate constants have thus far been completely determined only in normal conscious albino rats (Table 1). Partial analyses indicate that the values are quite similar in the conscious monkey (Kennedy et al., 1978).

The  $\lambda$ ,  $\Phi$ , and the enzyme kinetic constants are grouped together to constitute a single, lumped constant (Fig. 1B). It can be shown mathematically that this lumped constant is equal to the asymptotic value of the product of the ratio of the cerebral extraction ratios of [ $^{14}\text{C}$ ]DG and glucose and the ratio of the arterial blood to plasma-specific activities when the arterial plasma [ $^{14}\text{C}$ ]DG concentration is maintained constant (Sokoloff et al., 1977). The lumped constant is also determined in a separate group of animals from arterial and cerebral venous blood samples drawn during a programmed intravenous infusion which produces and maintains a constant arterial plasma [ $^{14}\text{C}$ ]DG concentration (Sokoloff et al., 1977). An example of such a determination in a conscious monkey is illustrated in Fig. 2. Thus far the lumped constant has been determined only in the albino rat, monkey, cat, and dog. The lumped constant appears to be characteristic of the species and does not appear to change significantly in a wide range of physiological conditions, some of which are shown in Table 2 (Sokoloff et al., 1977).

Despite its complex appearance, the operational equation is really nothing more than a general statement of the standard relationship by which rates of enzyme-catalyzed reactions are determined from measurements made with radioactive tracers (Fig. 1B). The numerator of the equation represents the amount of radioactive product formed in a given interval of time; it is equal to  $C_i^*$ , the combined concentrations of [ $^{14}\text{C}$ ]DG and [ $^{14}\text{C}$ ]DG-6-P in the tissue at time,  $T$ , measured by the quantitative autoradiographic technique, less a term that represents the free unmetabolized [ $^{14}\text{C}$ ]DG still remaining in the tissue. The denominator represents the integrated specific activity of the precursor pool multiplied by a factor, the lumped constant, which is equivalent to a correction factor for an isotope effect. The term with the exponential factor in the denominator takes into the account the lag in the

equilibration of the tissue precursor pool with the plasma.

### Experimental Procedure for Measurement of Local Cerebral Glucose Utilization

#### *Theoretical Considerations in the Design of the Procedure*

The operational equation of the method specifies the variables to be measured in order to determine  $R_i$ , the local rate of glucose consumption in the brain. The following variables are measured in each experiment: (1) the entire history of the arterial plasma [ $^{14}\text{C}$ ]DG concentration,  $C_p^*$ , from zero time to the time of killing,  $T$ ; (2) the steady-state arterial plasma glucose level  $C_p$ , over the same interval; and (3) the local concentration of  $^{14}\text{C}$  in the tissue at the time of killing,  $C_i^*(T)$ . The rate constants,  $k_1^*$ ,  $k_2^*$ , and  $k_3^*$ , and the lumped constant,  $\lambda V_m^* K_m / \Phi V_m K_m^*$ , are not measured in each experiment; the values for these constants that are used are those determined separately in other groups of animals as described above and presented in Tables 1 and 2.

The operational equation is generally applicable with all types of arterial plasma [ $^{14}\text{C}$ ]DG concentration curves. Its configuration, however, suggests that a declining curve approaching zero by the time of sacrifice is the choice to minimize certain potential errors. The quantitative autoradiographic technique measures only total  $^{14}\text{C}$  concentration in the tissue and does not distinguish between [ $^{14}\text{C}$ ]DG-6-P and [ $^{14}\text{C}$ ]DG. It is, however, the [ $^{14}\text{C}$ ]DG-6-P concentration that must be known to determine glucose consumption. [ $^{14}\text{C}$ ]DG-6-P concentration is calculated in the numerator of the operational equation, which equals the total tissue  $^{14}\text{C}$  content,  $C_i^*(T)$ , minus the [ $^{14}\text{C}$ ]DG concentration present in the tissue, estimated by the term containing the exponential factor and rate constants. In the denominator of the operational equation there is also a term containing an exponential factor and rate constants. Both these terms have the useful property of approaching zero with increasing time if  $C_p^*$  is also allowed to approach zero. The rate constants,  $k_1^*$ ,  $k_2^*$ , and  $k_3^*$ , are not measured in the same animals in which local glucose consumption is being measured. It is conceivable that the rate constants in Table 1 are not equally applicable in all physiological, pharmacological, and pathological states. One possible solution is to determine the rate constants for each condition to be studied. An al-

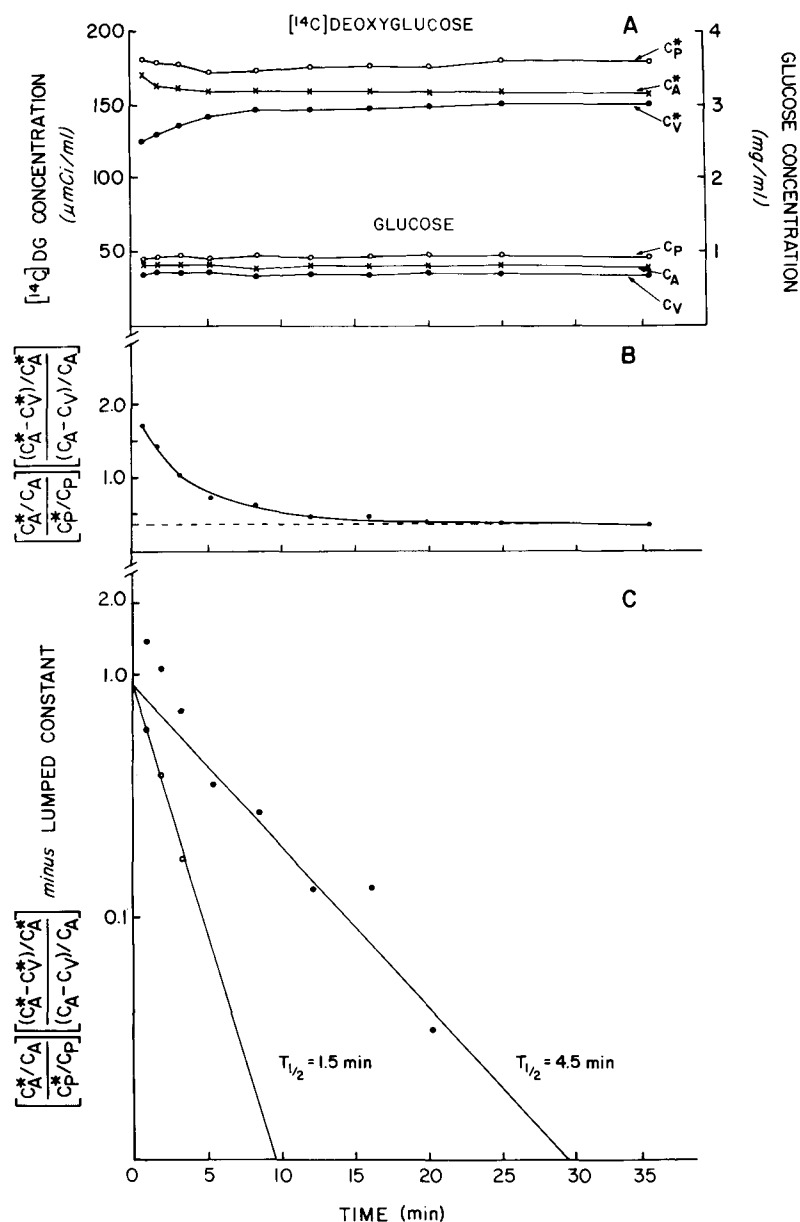


**FIG. 2.** Data obtained and their use in the determination of the lumped constant and the combination of rate constants,  $(k_2^* + k_3^*)$ , in a representative experiment. **A:** Time courses of arterial blood and plasma concentrations of  $[^{14}\text{C}]$ deoxyglucose ( $[^{14}\text{C}] \text{ DG}$ ) and glucose and cerebral venous blood concentrations of  $[^{14}\text{C}] \text{ DG}$  and glucose during programmed intravenous infusion of  $[^{14}\text{C}] \text{ DG}$ . **B:** Arithmetic plot of the function derived from the variables in A and combined as indicated in the formula on the ordinate against time. This function declines exponentially, with a rate constant equal to  $(k_2^* + k_3^*)$ , until it reaches an asymptotic value equal to the lumped constant, 0.35, in this experiment (dashed line). **C:** Semilogarithmic plot of the curve in B less the lumped constant, i.e., its asymptotic value. Solid circles represent actual values. This curve is analyzed into two components by a standard curve-peeling technique to yield the two straight lines representing the separate components. Open circles are points for the fast component, obtained by subtracting the values for the slow component from the solid circles. The rate constants for these two components represent the values of  $(k_2^* + k_3^*)$  for two compartments; the fast and slow compartments are assumed to represent gray and white matter, respectively. In this experiment the values for  $(k_2^* + k_3^*)$  were found to equal 0.462 (half-time = 1.5 min) and 0.154 (half-time = 4.5 min) in gray and white matter, respectively. (From Kennedy et al. 1978.)

ternative solution, and the one chosen, is to administer the  $[^{14}\text{C}] \text{ DG}$  as a single intravenous pulse at zero time and to allow sufficient time for the clearance of  $[^{14}\text{C}] \text{ DG}$  from the plasma and the terms containing the rate constants to fall to levels too low to influence the final result. To wait until these terms reach zero is impractical because of the long time required and the risk of effects of the small but finite rate of loss of  $[^{14}\text{C}] \text{ DG}$ -6-P from the tissues. A reasonable time interval is 45 minutes; by this time the plasma level has fallen to very low levels, and on the basis of the values of  $(k_2^* + k_3^*)$  in Table 1, the

exponential factors have declined through at least 10 half-lives.

### Experimental Protocol

The animals are prepared for the experiment by the insertion of polyethylene catheters in any convenient artery and vein. In the rat the femoral or the tail arteries and veins have been found satisfactory. In the monkey and cat the femoral vessels are probably most convenient. The catheters are inserted

TABLE 2. Values of the lumped constant in the albino rat, rhesus monkey, cat, and dog

Animal	No. of animals	Mean $\pm$ SD	SEM
Albino rat			
Conscious	15	0.464 $\pm$ 0.099 <sup>a</sup>	$\pm$ 0.026
Anesthetized	9	0.512 $\pm$ 0.118 <sup>a</sup>	$\pm$ 0.039
Conscious (5% CO <sub>2</sub> )	2	0.463 $\pm$ 0.122 <sup>a</sup>	$\pm$ 0.086
Combined	26	0.481 $\pm$ 0.119	$\pm$ 0.023
Rhesus monkey, conscious	7	0.344 $\pm$ 0.095	$\pm$ 0.036
Cat, anesthetized	6	0.411 $\pm$ 0.013	$\pm$ 0.005
Dog (beagle puppy), conscious	7	0.558 $\pm$ 0.082	$\pm$ 0.031

<sup>a</sup> No statistically significant difference between normal conscious and anesthetized rats ( $0.3 < p < 0.4$ ) and conscious rats breathing 5% CO<sub>2</sub> ( $p > 0.9$ ).

Note: The values were obtained as follows: rat, Sokoloff et al., 1977; monkey, Kennedy et al., 1978; cat, M. Miyaoka, J. Magnes, C. Kennedy, M. Shinohara, and L. Sokoloff, unpublished data; dog, Duffy et al., 1979. (From Sokoloff, 1979.)

under anesthesia, and anesthetic agents without long-lasting aftereffects should be used. Light halothane anesthesia with or without supplementation with nitrous oxide has been found to be quite satisfactory. At least 2 hours are allowed for recovery from the surgery and anesthesia before initiation of the experiment.

The design of the experimental procedure for the measurement of local cerebral glucose utilization was based on the theoretical considerations discussed above. At zero time a pulse of 125  $\mu$ Ci (no more than 2.5  $\mu$ moles) of [<sup>14</sup>C]DG per kilogram of body weight is administered to the animal via the venous catheter. Arterial sampling is initiated with the onset of the pulse, and timed 50–100  $\mu$ l samples of arterial blood are collected consecutively as rapidly as possible during the early period so as not to miss the peak of the arterial curve. Arterial sampling is continued at less frequent intervals later in the experimental period but at sufficient frequency to define fully the arterial curve. The arterial blood samples are immediately centrifuged to separate the plasma, which is stored on ice until assayed for [<sup>14</sup>C]DG by liquid scintillation counting and glucose concentrations by standard enzymatic methods. At approximately 45 minutes the animal is decapitated, and the brain is removed and frozen in Freon XII or isopentane maintained between  $-50$  and  $-75^{\circ}\text{C}$  with liquid nitrogen. When fully frozen, the brain is stored at  $-70^{\circ}\text{C}$  until sectioned and autoradiographed. The experimental period may be limited to 30 minutes. This is theoretically permissible and may sometimes be necessary for reasons of experi-

mental expediency, but greater errors due to possible inaccuracies in the rate constants may result.

#### Autoradiographic Measurement of Tissue <sup>14</sup>C Concentration

The <sup>14</sup>C concentrations in localized regions of the brain are measured by a modification of the quantitative autoradiographic technique previously described (Reivich et al., 1969). The frozen brain is coated with chilled embedding medium (Lipshaw Manufacturing Co., Detroit, Mich.) and fixed to object-holders appropriate to the microtome to be used.

Brain sections, precisely 20  $\mu$ m in thickness, are prepared in a cryostat maintained at  $-21$  to  $-22^{\circ}\text{C}$ . The brain sections are picked up on glass cover slips, dried on a hot plate at  $60^{\circ}\text{C}$  for at least 5 minutes, and placed sequentially in an X-ray cassette. A set of [<sup>14</sup>C]methyl methacrylate standards (Amersham Corp., Arlington Heights, Ill.), which include a blank and a series of progressively increasing <sup>14</sup>C concentrations, are also placed in the cassette. These standards must previously have been calibrated for their autoradiographic equivalence to the <sup>14</sup>C concentrations in brain sections, 20  $\mu$ m in thickness, prepared as described above. The method of calibration has been previously described (Reivich et al., 1969).

Autoradiographs are prepared from these sections directly in the X-ray cassette with Kodak single-coated, blue-sensitive Medical X-ray Film, Type SB-5 (Eastman Kodak Co., Rochester, N. Y.).

The exposure time is generally 5–6 days with the doses used as described above, and the exposed films are developed according to the instructions supplied with the film. The SB-5 X-ray film is rapid but coarse grained. For finer-grained autoradiographs and, therefore, better-defined images with higher resolution, it is possible to use mammographic films, such as DuPont LoDose or Kodak MR-1 films, or fine-grain panchromatic film such as Kodak Plus-X, but the exposure times are two to three times longer. The autoradiographs provide a pictorial representation of the relative  $^{14}\text{C}$  concentrations in the various cerebral structures and the plastic standards. A calibration curve of the relationship between optical density and tissue  $^{14}\text{C}$  concentration for each film is obtained by densitometric measurements of the portions of the film representing the various standards. The local tissue concentrations are then determined from the calibration curve and the optical densities of the film in the regions representing the cerebral structures of interest. Local cerebral glucose utilization is calculated from the local tissue concentrations of  $^{14}\text{C}$  and the plasma [ $^{14}\text{C}$ ]DG and glucose concentrations according to the operational equation (Fig. 1B).

#### *Computerized Color-Coded Image Processing*

The autoradiographs provide pictorial representations of only the relative concentrations of the isotope in the various tissues. Because of the use of a pulse followed by a long period before killing, the isotope is contained mainly in DG-6-P, which reflects the rate of glucose metabolism. The autoradiographs are, therefore, pictorial representations also of the relative but not the actual rates of glucose utilization in all the structures of the nervous system. Furthermore, the resolution of differences in relative rates is limited by the ability of the human eye to recognize differences in shades of gray. Manual densitometric analysis permits the computation of actual rates of glucose utilization with a fair degree of resolution, but it generates enormous tables of data which fail to convey the tremendous heterogeneity of metabolic rates, even within anatomic structures, or the full information contained within the autoradiographs. Goochee et al. (1980) have developed a computerized image-processing system to analyze and transform the autoradiographs into color-coded maps of the distribution of the actual rates of glucose utilization exactly where they are located throughout the central nervous system. The autoradiographs are

scanned automatically by a computer-controlled scanning microdensitometer. The optical density of each spot in the autoradiograph, from 25 to 100  $\mu\text{m}$ , as selected, is stored in a computer, converted to  $^{14}\text{C}$  concentration on the basis of the optical densities of the calibrated  $^{14}\text{C}$  plastic standards, and then converted to local rates of glucose utilization by solution of the operational equation of the method. Colors are assigned to narrow ranges of the rates of glucose utilization, and the autoradiographs are then displayed on a color TV monitor in color along with a calibrated color scale for identifying the rate of glucose utilization in each spot of the autoradiograph from its color. These color maps add a third dimension, the rate of glucose utilization on a color scale, to the spatial dimensions already present on the autoradiographs.

#### **Rates of Local Cerebral Glucose Utilization in the Normal Conscious State**

Thus far, quantitative measurements of local cerebral glucose utilization have been reported only for the albino rat (Sokoloff et al., 1977) and monkey (Kennedy et al., 1978). These values are presented in Table 3. The rates of local cerebral glucose utilization in the normal conscious rat vary widely throughout the brain. The values in white structures tend to group together and are always considerably below those of gray structures. The average value in gray matter is approximately three times that of white matter, but the individual values vary from approximately 50 to 200  $\mu\text{moles}$  of glucose/100 g/min. The highest values are in the structures involved in auditory functions, with the inferior colliculus clearly the most metabolically active structure in the brain.

The rates of local cerebral glucose utilization in the conscious monkey exhibit similar heterogeneity, but they are generally one-third to one-half the values in corresponding structures of the rat brain (Table 3). The differences in rates in the rat and monkey brain are consistent with the different cellular packing densities in the brains of these two species.

#### **Effects of General Anesthesia**

General anesthesia produced by thiopental reduces the rates of glucose utilization in all structures of the rat brain (Table 4) (Sokoloff et al., 1977). The effects are not uniform, however. The greatest reductions occur in the gray structures,

**TABLE 3.** Representative values for local cerebral glucose utilization in the normal conscious albino rat and monkey

Structure	Local cerebral glucose utilization ( $\mu$ moles/100 g/min)	
	Albino rat <sup>a</sup> (n = 10)	Monkey <sup>b</sup> (n = 7)
<b>Gray Matter</b>		
Visual cortex	107 $\pm$ 6	59 $\pm$ 2
Auditory cortex	162 $\pm$ 5	79 $\pm$ 4
Parietal cortex	112 $\pm$ 5	47 $\pm$ 4
Sensorimotor cortex	120 $\pm$ 5	44 $\pm$ 3
Thalamus		
Lateral nucleus	116 $\pm$ 5	54 $\pm$ 2
Ventral nucleus	109 $\pm$ 5	43 $\pm$ 2
Medial geniculate body	131 $\pm$ 5	65 $\pm$ 3
Lateral geniculate body	96 $\pm$ 5	39 $\pm$ 1
Hypothalamus	54 $\pm$ 2	25 $\pm$ 1
Mamillary body	121 $\pm$ 5	57 $\pm$ 3
Hippocampus	79 $\pm$ 3	39 $\pm$ 2
Amygdala	52 $\pm$ 2	25 $\pm$ 2
Caudate-putamen	110 $\pm$ 4	52 $\pm$ 3
Nucleus accumbens	82 $\pm$ 3	36 $\pm$ 2
Globus-pallidus	58 $\pm$ 2	26 $\pm$ 2
Substantia nigra	58 $\pm$ 3	29 $\pm$ 2
Vestibular nucleus	128 $\pm$ 5	66 $\pm$ 3
Cochlear nucleus	113 $\pm$ 7	51 $\pm$ 3
Superior olivary nucleus	133 $\pm$ 7	63 $\pm$ 4
Inferior colliculus	197 $\pm$ 10	103 $\pm$ 6
Superior colliculus	95 $\pm$ 5	55 $\pm$ 4
Pontine gray matter	62 $\pm$ 3	28 $\pm$ 1
Cerebellar cortex	57 $\pm$ 2	31 $\pm$ 2
Cerebellar nuclei	100 $\pm$ 4	45 $\pm$ 2
<b>White Matter</b>		
Corpus callosum	40 $\pm$ 2	11 $\pm$ 1
Internal capsule	33 $\pm$ 2	13 $\pm$ 1
Cerebellar white matter	37 $\pm$ 2	12 $\pm$ 1

<sup>a</sup> From Sokoloff et al., 1977.

<sup>b</sup> From Kennedy et al., 1978.

The values are the means  $\pm$  standard errors from measurements made in the number of animals indicated in parentheses.

particularly those of the primary sensory pathways. The effects in white matter, though definitely present, are relatively small compared to those of gray matter. These results are in agreement with those of previous studies in which anesthesia has been found to decrease the cerebral metabolic rate of the brain as a whole (Kety, 1950; Lassen, 1959; Sokoloff, 1976).

#### Relation Between Local Functional Activity and Energy Metabolism

The results of a variety of applications of the method demonstrate a clear relationship between local cerebral functional activity and glucose consumption. The most striking demonstrations of the close coupling between function and energy metabolism are seen with experimentally induced

**TABLE 4.** Effects of thiopental anesthesia on local cerebral glucose utilization in the rat<sup>a</sup>

Structure	Local cerebral glucose utilization <sup>b</sup> ( $\mu$ moles/100 g/min)		
	Control (n = 6)	Anesthetized (n = 8)	Change (%)
<b>Gray Matter</b>			
Visual cortex	111 $\pm$ 5	64 $\pm$ 3	-42
Auditory cortex	157 $\pm$ 5	81 $\pm$ 3	-48
Parietal cortex	107 $\pm$ 3	65 $\pm$ 2	-39
Sensorimotor cortex	118 $\pm$ 3	67 $\pm$ 2	-43
Lateral geniculate body	92 $\pm$ 2	53 $\pm$ 3	-42
Medial geniculate body	126 $\pm$ 6	63 $\pm$ 3	-50
Thalamus			
Lateral nucleus	108 $\pm$ 3	58 $\pm$ 2	-46
Ventral nucleus	98 $\pm$ 3	55 $\pm$ 1	-44
Hypothalamus	63 $\pm$ 3	43 $\pm$ 2	-32
Caudate-putamen	111 $\pm$ 4	72 $\pm$ 3	-35
Hippocampus: Ammon's horn	79 $\pm$ 1	56 $\pm$ 1	-29
Amygdala	56 $\pm$ 4	41 $\pm$ 2	-27
Cochlear nucleus	124 $\pm$ 7	79 $\pm$ 5	-36
Lateral lemniscus	114 $\pm$ 7	75 $\pm$ 4	-34
Inferior colliculus	198 $\pm$ 7	131 $\pm$ 8	-34
Superior olivary nucleus	141 $\pm$ 5	104 $\pm$ 7	-26
Superior colliculus	99 $\pm$ 3	59 $\pm$ 3	-40
Vestibular nucleus	133 $\pm$ 4	81 $\pm$ 4	-39
Pontine gray matter	69 $\pm$ 3	46 $\pm$ 3	-33
Cerebellar cortex	66 $\pm$ 2	44 $\pm$ 2	-33
Cerebellar nucleus	106 $\pm$ 4	75 $\pm$ 4	-29
<b>White Matter</b>			
Corpus callosum	42 $\pm$ 2	30 $\pm$ 2	-29
Genu of corpus callosum	35 $\pm$ 5	30 $\pm$ 2	-14
Internal capsule	35 $\pm$ 2	29 $\pm$ 2	-17
Cerebellar white matter	38 $\pm$ 2	29 $\pm$ 2	-24

<sup>a</sup> Determined at 30 minutes following pulse of [<sup>14</sup>C]deoxyglucose.

<sup>b</sup> The values are the means  $\pm$  standard errors obtained in the number of animals indicated in parentheses. All the differences are statistically significant at the  $p < 0.05$  level.

From Sokoloff et al., 1977.

local alterations in functional activity that are restricted to a few specific areas in the brain. The effects on local glucose consumption are then so pronounced that they are not only observed in the quantitative results, but can be visualized directly on the autoradiographs—which are really pictorial representations of the relative rates of glucose utilization in the various structural components of the brain.

#### Effects of Increased Functional Activity

**Effects of sciatic nerve stimulation.** Electrical stimulation of one sciatic nerve in the rat under barbiturate anesthesia causes pronounced increases in

glucose consumption (i.e., increased optical density in the autoradiographs) in the ipsilateral dorsal horn of the lumbar spinal cord (Kennedy et al., 1975).

**Effects of experimental focal seizures.** The local injection of penicillin into the hand-face area of the motor cortex of the Rhesus monkey has been shown to induce electrical discharges in the adjacent cortex and to result in recurrent focal seizures involving the face, arm, and hand on the contralateral side (Caveness, 1969). Such seizure activity causes selective increases in glucose consumption in areas of motor cortex adjacent to the penicillin locus and in small discrete regions of the putamen, globus

pallidus, caudate nucleus, thalamus, and substantia nigra of the same side (Fig. 3) (Kennedy et al., 1975). Similar studies in the rat have led to comparable results and provided evidence on the basis of an evoked metabolic response of a "mirror" focus in the motor cortex contralateral to the penicillin-induced epileptogenic focus (Collins et al., 1976).

#### *Effects of Decreased Functional Activity*

Decrements in functional activity result in reduced rates of glucose utilization. These effects are particularly striking in the auditory and visual

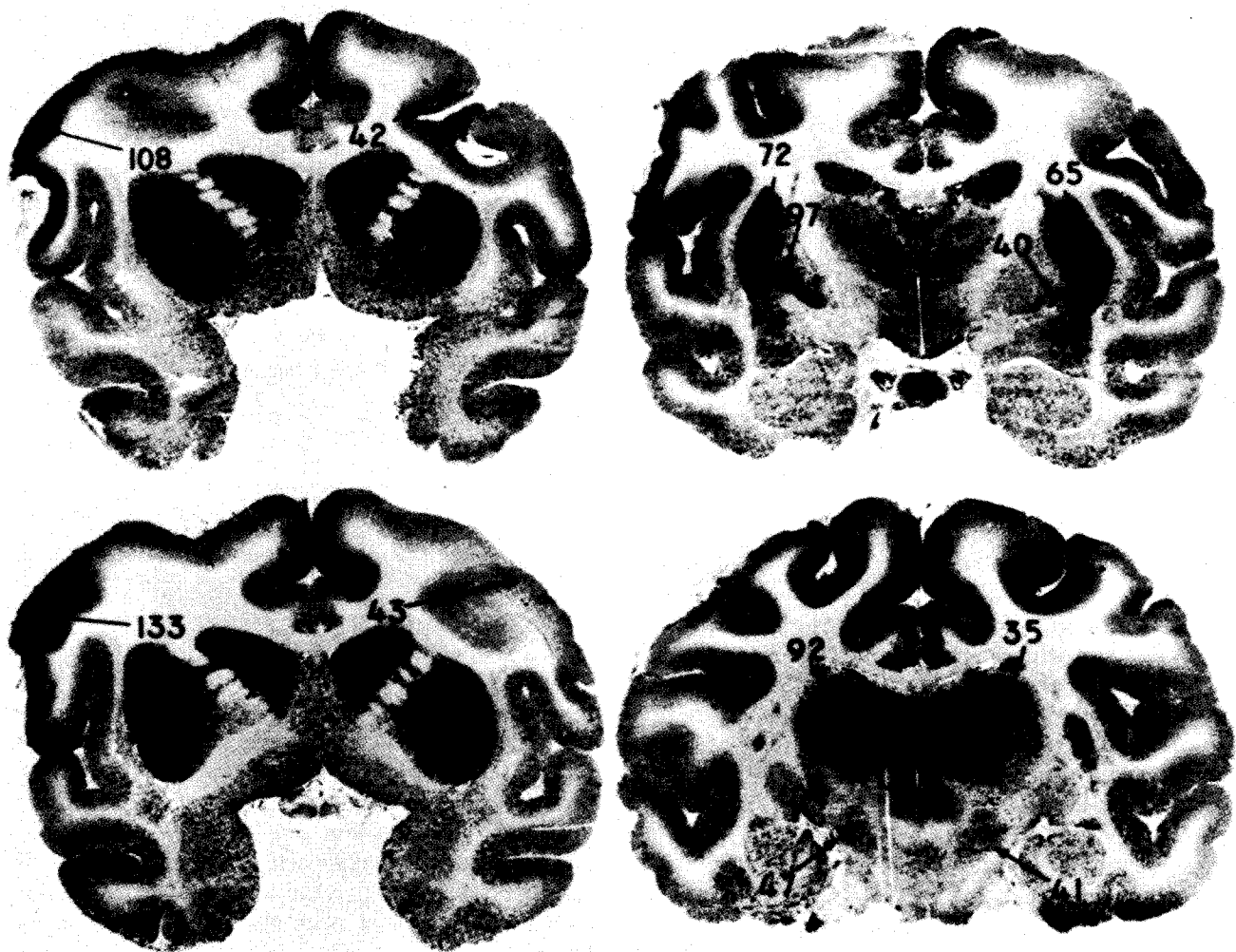


**FIG. 3.** Effects of focal seizures produced by local application of penicillin to motor cortex on local cerebral glucose utilization in the Rhesus monkey. The penicillin was applied to the hand and face area of the left motor cortex. The left side of the brain is on the left in each of the autoradiographs in the figure. The numbers are the rates of local cerebral glucose utilization in  $\mu\text{moles}/100\text{ g tissue}/\text{min}$ . Note the following: in the **upper left**, motor cortex in the region of penicillin application and corresponding region of contralateral motor cortex; **lower left**: ipsilateral and contralateral motor cortical regions remote from area of penicillin applications; **upper right**: ipsilateral and contralateral putamen and globus pallidus; **lower right**: ipsilateral and contralateral thalamic nuclei and substantia nigra. (From Sokoloff, 1977.)

systems of the rat and the visual system of the monkey.

**Effects of auditory deprivation.** In the albino rat some of the highest rates of local cerebral glucose utilization are found in components of the auditory system, i.e., auditory cortex, medial geniculate ganglion, inferior colliculus, lateral lemniscus, superior olive, and cochlear nucleus (Table 3). Bilateral auditory deprivation by occlusion of both external auditory canals with wax markedly depresses the metabolic activity in all of these areas (Sokoloff, 1977). The reductions are symmetrical bilaterally and range from 35 to 60%. Unilateral auditory deprivation also depresses the glucose consumption of these structures but to a lesser degree, and some of the structures are asymmetrically affected. For example, the metabolic activity of the ipsilateral cochlear nucleus equals 75% of the activity of the contralateral nucleus. The lateral lemniscus, superior olive, and medial geniculate ganglion are slightly lower on the contralateral side, while the contralateral inferior colliculus is markedly lower in metabolic activity than the ipsilateral structure. These results demonstrate that there is some degree of lateralization and crossing of auditory pathways in the rat.

**Visual deprivation in the rat.** In the rat, the visual system is 80–85% crossed at the optic chiasma (Lashley, 1934; Montero and Guillery, 1968), and unilateral enucleation removes most of the visual input to the central visual structures of the contralateral side. In the conscious rat studied 2–24 hours after unilateral enucleation, there are marked decrements in glucose utilization in the contralateral superior colliculus, lateral geniculate ganglion, and visual cortex as compared to the ipsilateral side (Kennedy et al., 1975).

**Visual deprivation in the monkey.** In animals with binocular visual systems, such as the Rhesus monkey, there is only approximately 50% crossing of the visual pathways, and the structures of the visual system on each side of the brain receive equal inputs from both retinæ. Although each retina projects more or less equally to both hemispheres, their projections remain segregated and terminate in six well-defined laminae in the lateral geniculate ganglia, three each for the ipsilateral and contralateral eyes (Hubel and Wiesel, 1968, 1972; Wiesel et al., 1974; Rakic, 1976). This segregation is preserved in the optic radiations which project the monocular representations of the two eyes for any segment of the visual field to adjacent regions of Layer IV of

the striate cortex (Hubel and Wiesel, 1968, 1972). The cells responding to the input of each monocular terminal zone are distributed transversely through the thickness of the striate cortex, resulting in a mosaic of columns, 0.3–0.5 mm in width, alternately representing the monocular inputs of the two eyes. The nature and distribution of these ocular dominance columns have previously been characterized by electrophysiological techniques (Hubel and Wiesel, 1968), Nauta degeneration methods (Hubel and Wiesel, 1972), and by autoradiographic visualization of axonal and transneuronal transport of [<sup>3</sup>H]proline- and [<sup>3</sup>H]fucose-labeled protein and/or glycoprotein (Wiesel et al., 1974; Rakic, 1976). Bilateral or unilateral visual deprivation, either by enucleation or by the insertion of opaque plastic discs, produces consistent changes in the pattern of distribution of the rates of glucose consumption, all clearly visible in the autoradiographs, that coincide closely with the changes in functional activity expected from known physiological and anatomical properties of the binocular visual system (Kennedy et al., 1976).

In animals with intact binocular vision, no bilateral asymmetry is seen in the autoradiographs of the structures of the visual system (Figs. 4A, 5A). The lateral geniculate ganglia and oculomotor nuclei appear to be of fairly uniform density and essentially the same on both sides (Fig. 4A). The visual cortex is also the same on both sides (Fig. 5A), but throughout all of Area 17 there is heterogeneous density distributed in a characteristic laminar pattern. These observations indicate that in animals with binocular visual input the rates of glucose consumption in the visual pathways are essentially equal on both sides of the brain and relatively uniform in the oculomotor nuclei and lateral geniculate ganglia, but markedly different in the various layers of the striate cortex.

Autoradiographs from animals with both eyes occluded exhibit generally decreased labeling of all components of the visual system, but the bilateral symmetry is fully retained (Figs. 4B, 5B), and the density within each lateral geniculate body is for the most part fairly uniform (Fig. 4B). In the striate cortex, however, the marked differences in the densities of the various layers seen in the animals with intact bilateral vision (Fig. 5A) are virtually absent so that, except for a faint delineation of a band within Layer IV, the concentration of the label is essentially homogeneous throughout the striate cortex (Fig. 5B).



5.0mm

**FIG. 4.** Autoradiography of coronal brain sections of monkey at the level of the lateral geniculate bodies. Large arrows point to the lateral geniculate bodies; small arrows point to oculomotor nuclear complex. **A:** Animal with intact binocular vision. Note the bilateral symmetry and relative homogeneity of the lateral geniculate bodies and oculomotor nuclei. **B:** Animal with bilateral visual occlusion. Note the reduced relative densities, the relative homogeneity, and the bilateral symmetry of the lateral geniculate bodies and oculomotor nuclei. **C:** Animal with right eye occluded. The left side of the brain is on the left side of the photograph. Note the laminae and the inverse order of the dark and light bands in the two lateral geniculate bodies. Note also the lesser density of the oculomotor nuclear complex on the side contralateral to the occluded eye. (From Kennedy et al., 1976.)

Autoradiographs from monkeys with only monocular input because of unilateral visual occlusion exhibit markedly different patterns from those described above. Both lateral geniculate bodies exhibit exactly inverse patterns of alternating dark and light bands corresponding to the known laminae representing the regions receiving the different inputs from the retinæ of the intact and occluded eyes (Fig. 4C). Bilateral asymmetry is also seen in the oculomotor nuclear complex; a lower density is apparent in the nuclear complex contralateral to the occluded eye (Fig. 4C). In the striate cortex the pattern of distribution of [ $^{14}\text{C}$ ]DG-6-P appears to be a composite of the patterns seen in the animals with intact and bilaterally occluded visual input. The pattern found in the former regularly alternates with that of the latter in columns oriented perpendicularly to the cortical surface (Fig. 5C). The dimensions, arrangement, and distribution of these columns are identical to those of the ocular dominance columns described by Hubel and Wiesel (Hubel and Wiesel, 1968, 1972; Wiesel et al., 1974). These columns reflect the interdigitation of the representations of the two retinæ in the visual cortex. Each element in the visual fields is represented by a pair of contiguous bands in the visual cortex, one for each of the two retinæ or their portions that correspond to the given point in the visual fields. With symmetrical visual input bilaterally, the columns representing the two eyes are equally active and, therefore, not visualized in the autoradiographs (Fig. 5A). When one eye is blocked, however, only those columns representing the blocked eye become metabolically less active, and the autoradiographs then display the alternate bands of normal and depressed activities corresponding to the regions of visual cortical representation of the two eyes (Fig. 5C).

There can be seen in the autoradiographs from the animals with unilateral visual deprivation a pair of regions in the folded calcarine cortex that exhibit bilateral asymmetry (Fig. 5C). The ocular dominance columns are absent on both sides, but on the side contralateral to the occluded eye this region has the appearance of visual cortex from an animal with normal bilateral vision, and on the ipsilateral side this region looks like cortex from an animal with both eyes occluded (Fig. 5). These regions are the loci of the cortical representation of the blind spots of the visual fields and normally have only monocular input (Kennedy et al., 1975, 1976). The area of the optic disc in the nasal half of each retina

cannot transmit to this region of the contralateral striate cortex which, therefore, receives its sole input from an area in the temporal half of the ipsilateral retina. Occlusion of one eye deprives this region of the ipsilateral striate cortex of all input while the corresponding region of the contralateral striate cortex retains uninterrupted input from the intact eye. The metabolic reflection of this ipsilateral monocular input is seen in the autoradiograph in Fig. 5C.

The results of these studies with the [ $^{14}\text{C}$ ]deoxyglucose method in the binocular visual system of the monkey represent the most dramatic demonstration of the close relationship between physiological changes in functional activity and the rate of energy metabolism in specific components of the central nervous system.

#### Applications of the Deoxyglucose Method

The results of studies like those described above on the effects of experimentally induced focal alterations of functional activity on local glucose utilization have demonstrated a close coupling between local functional activity and energy metabolism in the central nervous system. The effects are often so pronounced that they can be visualized directly on the autoradiographs, which provide pictorial representations of the relative rates of glucose utilization throughout the brain. This technique of autoradiographic visualization of evoked metabolic responses offers a powerful tool to map functional neural pathways simultaneously in all anatomical components of the central nervous system, and extensive use has been made of it for this purpose (Plum et al., 1976). The results have clearly demonstrated the effectiveness of metabolic responses, either positive or negative, in identifying regions of the central nervous system involved in specific functions.

The method has been used most extensively in qualitative studies in which regions of altered functional activity are identified by the change in their visual appearance relative to other regions in the autoradiographs. Such qualitative studies are effective only when the effects are lateralized to one side or when only a few discrete regions are affected; other regions serve as the controls. Quantitative comparisons cannot, however, be made for equivalent regions between two or more animals. To make quantitative comparisons between animals, the fully quantitative method must be used, which takes into account the various factors, particularly

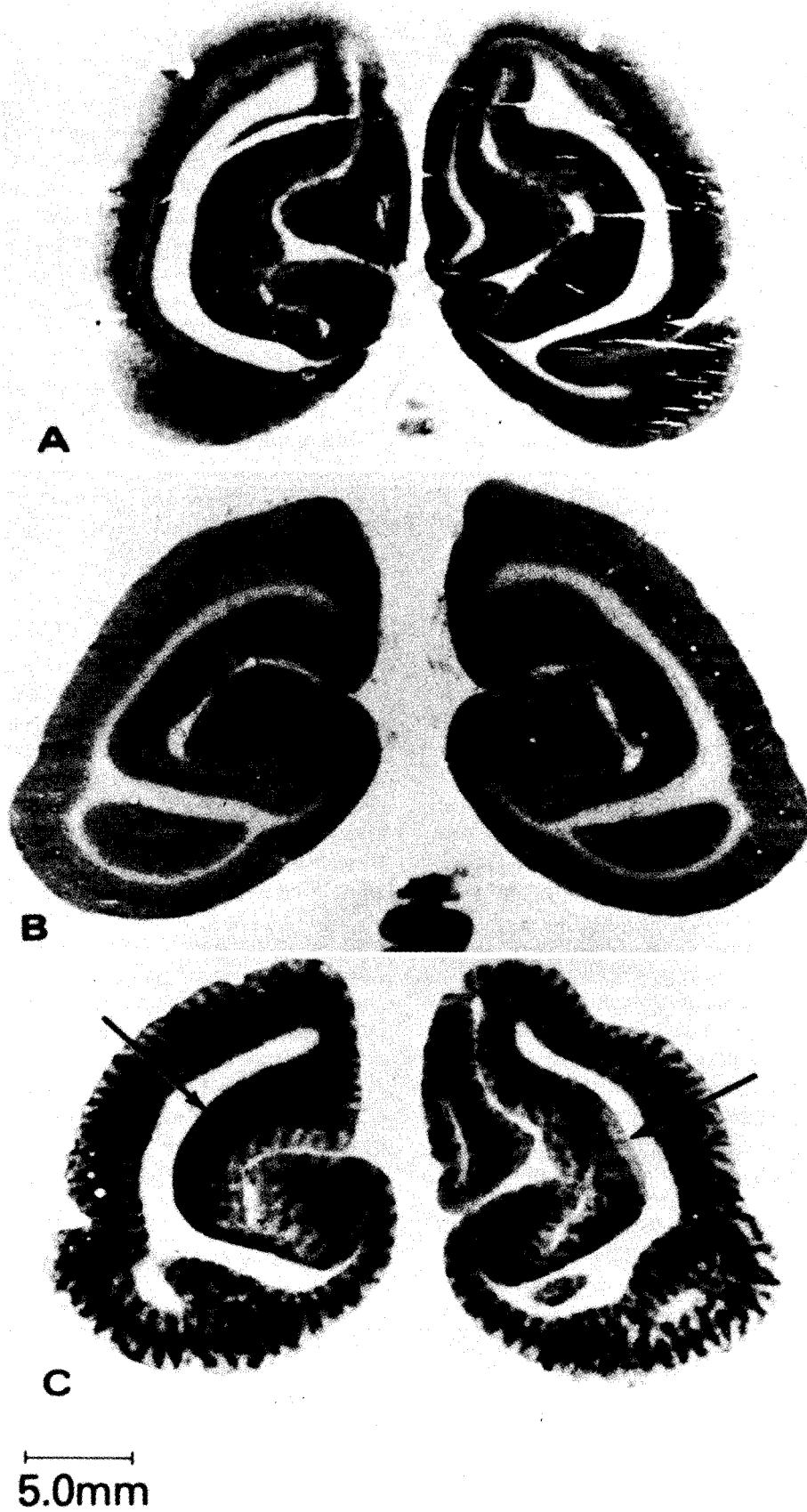


FIG. 5. (See facing page for legend.)

the plasma glucose level, that influence the magnitude of labeling of the tissue. The method must be used quantitatively when the experimental procedure produces systemic effects and alters metabolism in many regions of the brain.

A comprehensive review of the many qualitative and quantitative applications of the method is beyond the scope of this report. Only some of the many neurophysiological, neuroanatomical, pharmacological, and pathophysiological applications of the method will be briefly noted merely to illustrate the broad extent of its potential usefulness.

#### *Neurophysiological and Neuroanatomical Applications*

Many of the physiological applications of the [<sup>14</sup>C]deoxyglucose method were in studies designed to test the method and to examine the relationship between local cerebral functional and metabolic activities. These applications have been described above. The most dramatic results have been obtained in the visual systems of the monkey and the rat. The method has, for example, been used to define the nature, conformation, and distribution of the ocular dominance columns in the striate cortex of the monkey (Fig. 5C) (Kennedy et al., 1976). It has been used by Hubel et al. (1978) to do the same for the orientation columns in the striate cortex of the monkey. A byproduct of the studies of the ocular dominance columns was the identification of the loci of the visual cortical representation of the blind spots of the visual fields (Fig. 5C) (Kennedy et al., 1976). Studies are currently in progress to map the pathways of higher visual functions beyond the striate cortex; the results thus far demonstrate extensive areas of involvement of the inferior temporal cortex in visual processing (Jarvis et al., 1978). Des Rosiers et al. (1978) have used the method to demonstrate functional plasticity in the striate cortex of the infant monkey. The ocular dominance columns are already present on the first day of life, but if one eye is kept patched for three months, the columns representing the open eye broaden and completely take over the adjacent regions of cortex containing the columns for the eye

that had been patched. Inasmuch as there is no longer any cortical representation for the patched eye, the animal becomes functionally blind in one eye. This phenomenon is almost certainly the basis for the cortical blindness or amblyopia that often occurs in children with uncorrected strabismus.

There have also been extensive studies of the visual system of the rat. This species has little if any binocular vision and, therefore, lacks the ocular dominance columns. Batipps et al. (1981) have compared the rates of local cerebral glucose utilization in albino and Norway brown rats during exposure to ambient light. The rates in the two strains were essentially the same throughout the brain except in the components of the primary visual system. The metabolic rates in the superior colliculus, lateral geniculate, and visual cortex of the albino rat were significantly lower than those in the pigmented rat. Miyaoka et al. (1979a) have studied the influence of the intensity of retinal stimulation with randomly spaced light flashes on the metabolic rates in the visual systems of the two strains. In dark-adapted animals there is relatively little difference between the two strains. With increasing intensity of light, the rates of glucose utilization first increase in the primary projection areas of the retina, e.g., superficial layer of the superior colliculus and lateral geniculate body, and the slopes of the increase are steeper in the albino rat (Fig. 6). At 7 lux, however, the metabolic rates peak in the albino rat and then decrease with increasing light intensity. In contrast, the metabolic rates in the pigmented rat rise until they reach a plateau at about 700 lux, approximately the ambient light intensity in the laboratory. At this level, the metabolic rates in the visual structures of the albino rat are considerably below those of the pigmented rat. These results are consistent with the greater intensity of light reaching the visual cells of the retina in the albino rats because of lack of pigment and the subsequent damage to the rods at higher light intensities. It is of considerable interest that the rates of glucose utilization in these visual structures obey the Weber-Fechner Law, i.e., the metabolic rate is directly proportional to the logarithm of the intensity of stimulation (Miyaoka et al., 1979a). Inasmuch as

**FIG. 5.** Autoradiographs of coronal brain sections from Rhesus monkeys at the level of the striate cortex. **A:** Animal with normal binocular vision. Note the laminar distribution of the density; the dark band corresponds to Layer IV. **B:** Animal with bilateral visual deprivation. Note the almost uniform and reduced relative density, especially the virtual disappearance of the dark band corresponding to Layer IV. **C:** Animal with right eye occluded. The half-brain on the left side of the photograph represents the left hemisphere contralateral to the occluded eye. Note the alternate dark and light striations, each approximately 0.3–0.4 mm in width, that represent the ocular dominance columns. These columns are most apparent in the dark band corresponding to Layer IV but extend through the entire thickness of the cortex. The arrows point to regions of bilateral asymmetry where the ocular dominance columns are absent. These are presumably areas with normally only monocular input. The one on the left, contralateral to occluded eye, has a continuous dark lamina corresponding to Layer IV which is completely absent on the side ipsilateral to the occluded eye. These regions are believed to be the loci of the cortical representations of the blind spots. (From Kennedy et al., 1976.)

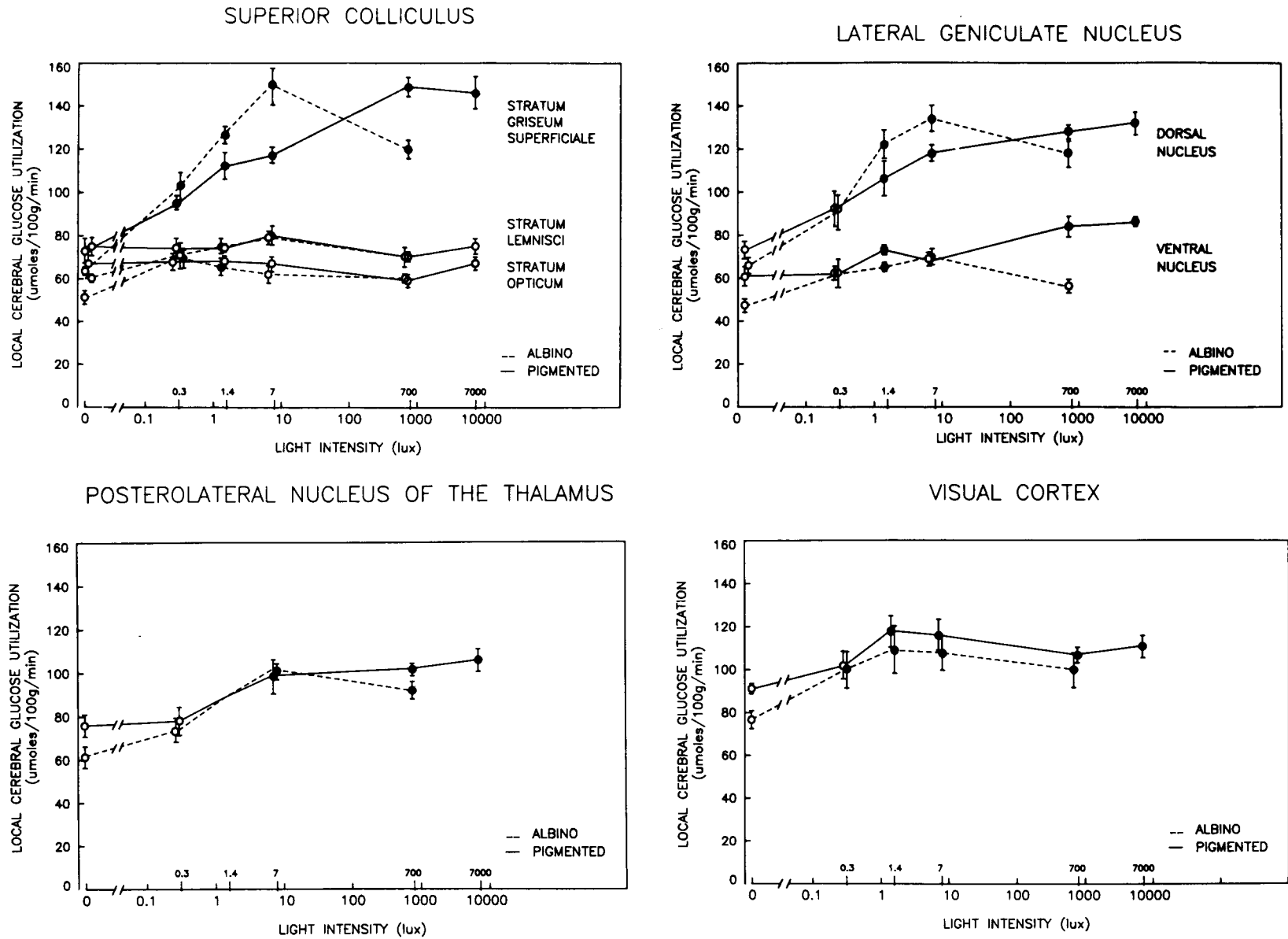


**FIG. 6.** Effects of intensity of retinal illumination with randomly spaced light flashes on local cerebral glucose utilization in components of the visual system of the albino and Norway brown rat. Note that the local glucose utilization is proportional to the logarithm of the intensity of illumination, at least at lower levels of intensity, in the primary projection areas of the retina. (From Miyaoka et al., 1979a.)

this law was first developed from behavioral manifestations, these results imply that there is a quantitative relationship between behavioral and metabolic responses.

Although less extensive, there have also been applications of the method to other sensory systems. In studies of the olfactory system Sharp et al. (1975) have found that olfactory stimulation with specific odors activates glucose utilization in localized regions of the olfactory bulb. In addition to the experiments in the auditory system described above, there have been studies of tonotopic representation in the auditory system. Webster et al. (1978) have obtained clear evidence of selective regions of metabolic activation in the cochlear nucleus, superior olivary complex, nuclei of the lateral lemnisci, and the inferior colliculus in cats in response to different frequencies of auditory stimulation. Similar results have been obtained by Silverman et al. (1977) in the rat and guinea pig. Studies of the sensory cortex have demonstrated metabolic activation of the "whisker barrels" by stimulation of the vibrissae in the rat (Durham and Woolsey, 1977; Hand et al., 1978). Each vibrissa is represented in a discrete region of the sensory cortex; their precise location and extent have been elegantly mapped by Hand et al. (1978) and Hand (1981) by means of the [ $^{14}\text{C}$ ]deoxyglucose method.

Thus far, there has been relatively little application of the method to the physiology of motor functions. Kennedy et al. (1980) have studied monkeys that were conditioned to perform a task with one hand in response to visual cues; in the monkeys which were performing, they observed metabolic activation throughout the appropriate areas of the motor as well as sensory systems from the cortex to the spinal cord.

An interesting physiological application of the [ $^{14}\text{C}$ ]deoxyglucose method has been to the study of circadian rhythms in the central nervous system. Schwartz and his co-workers (1977, 1980) found that the suprachiasmatic nucleus in the rat exhibits circadian rhythmicity in metabolic activity, high during the day and low during the night (Fig. 7). None of the other structures in the brain that they examined showed rhythmic activity. The normally low activity present in the nucleus in the dark could be markedly increased by light, but darkness did not reduce the glucose utilization during the day. The rhythm is entrained to light; reversal of the light-dark cycle leads not only to reversal of the rhythm in running activity, but also in the cycle of

metabolic activity in the suprachiasmatic nucleus. These studies lend support to a role of the suprachiasmatic nucleus in the organization of circadian rhythms in the central nervous system.

Much of our knowledge of neurophysiology has been derived from studies of the electrical activity of the nervous system. Indeed, from the heavy emphasis that has been placed on electrophysiology one might gather that the brain is really an electric organ rather than a chemical one that functions mainly by the release of chemical transmitters at synapses. Nevertheless, electrical activity is unquestionably fundamental to the process of conduction, and it is appropriate to inquire how the local metabolic activities revealed by the [ $^{14}\text{C}$ ]deoxyglucose method are related to the electrical activity of the nervous system. This question is currently being examined by Yarowsky and his co-workers (1979) in the superior cervical ganglion of the rat. The advantage of this structure is that its preganglionic input and postganglionic output can be isolated and electrically stimulated and/or monitored *in vivo*. The results thus far indicate a clear relationship between electrical input to the ganglion and its metabolic activity. In normal conscious rats its rate of glucose utilization equals approximately  $35 \mu\text{moles}/100 \text{ g}/\text{min}$ . This rate is markedly depressed by anesthesia or denervation and enhanced by electrical stimulation of the afferent nerves. The metabolic activation is frequency dependent in the range of 5–15 Hz, increasing linearly in magnitude with increasing frequency of the stimulation (Fig. 8). Similar effects of electrical stimulation on the oxygen and glucose consumption of the excised ganglion studied *in vitro* have been observed (Horowicz and Larrabee, 1958; Larrabee, 1958; Friedli, 1978). Recent studies have also shown that antidromic stimulation of the postganglionic efferent pathways from the ganglion has similar effects; stimulation of the external carotid nerve antidromically activates glucose utilization in the region of distribution of the cell bodies of this efferent pathway, indicating that not only the preganglionic axonal terminals are metabolically activated, but the postganglionic cell bodies as well (Yarowsky et al., 1980). As already demonstrated in the neurohypophysis (Mata et al., 1980), the effects of electrical stimulation on energy metabolism in the superior cervical ganglion are also probably due to the ionic currents associated with the spike activity and the consequent activation of the  $\text{Na}^+$ ,  $\text{K}^+$ -ATPase activity to restore the ionic gradients.

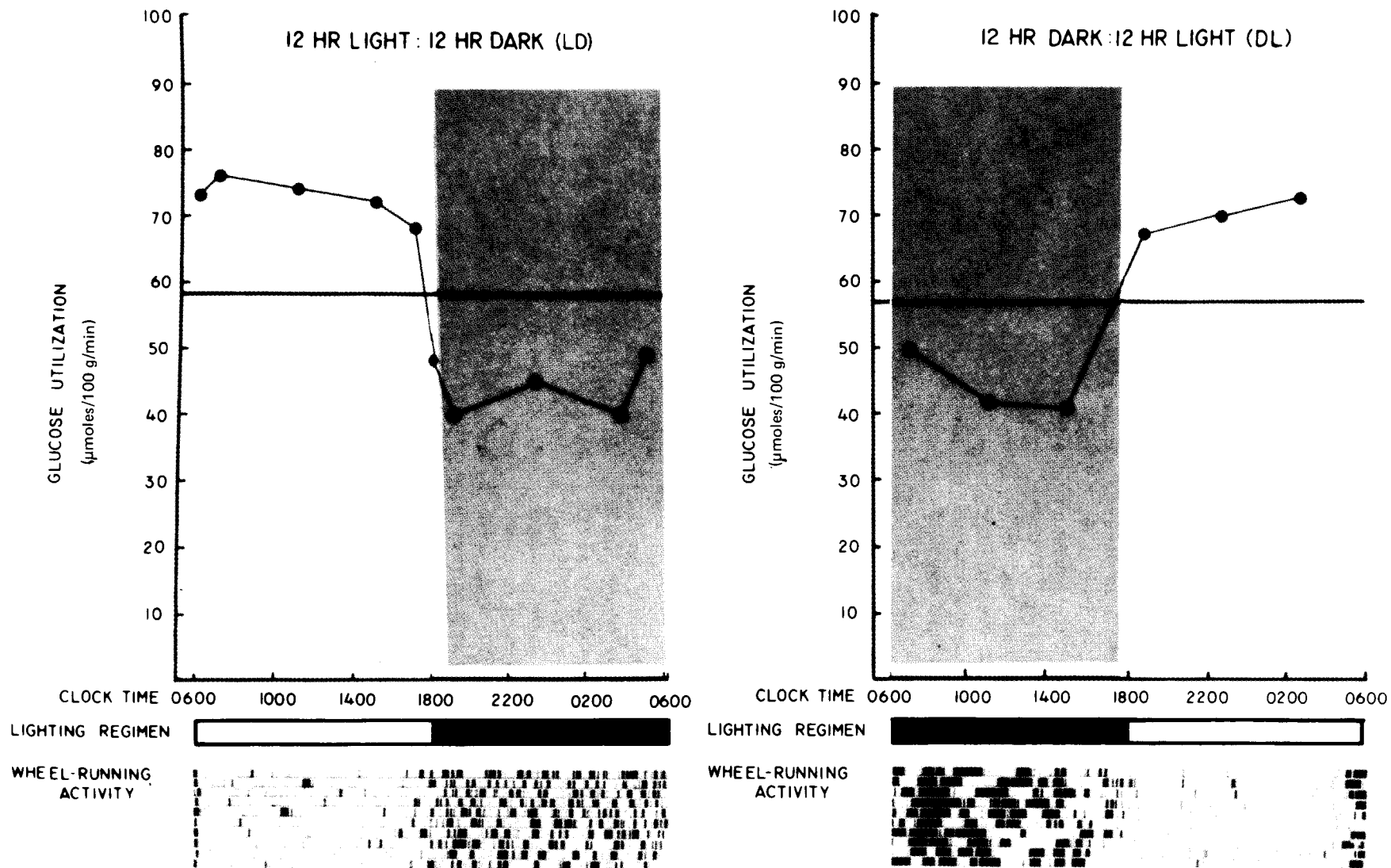
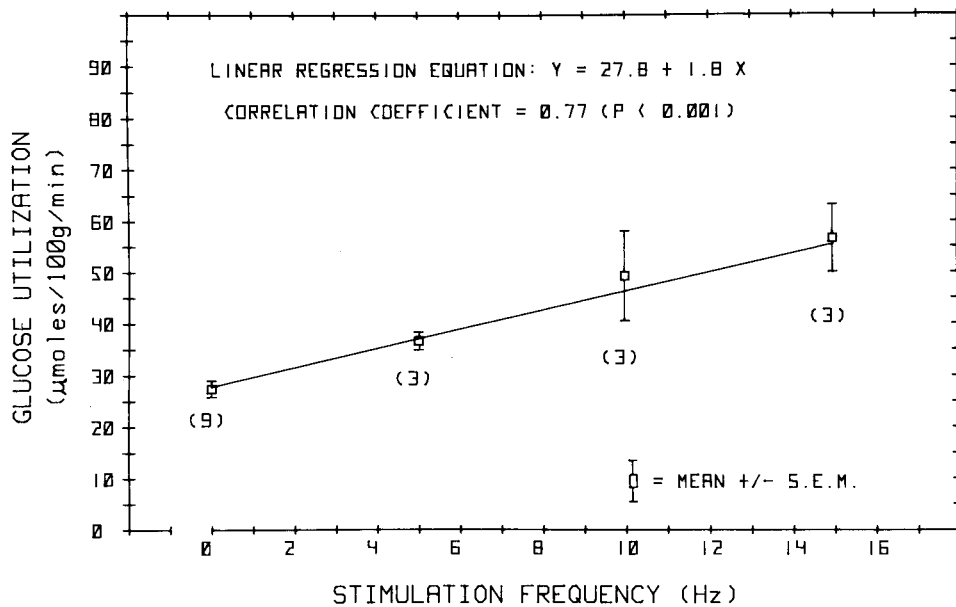


FIG. 7. Circadian rhythm in glucose utilization in suprachiasmatic nucleus in the rat. **Left:** Animals entrained to 12 hours of light during day and 12 hours of darkness during night. **Right:** Animals entrained to the opposite light-dark regimen. (From Schwartz et al., 1980.)



**FIG. 8.** Relationship between average glucose utilization in the superior cervical ganglion of the rat and the frequency of electrical stimulation of the cervical sympathetic trunk, (i.e., preganglionic input). The animals were under urethane anesthesia. The cervical sympathetic trunk was transected, and the distal portion was stimulated with 0.3–0.4 msec monopolar pulses administered via a stimulation isolation unit at a maximum current of 500  $\mu$ A and at the frequency indicated. (From Yarowsky et al., 1979.)

Electrical stimulation of the afferents to sympathetic ganglia have been shown to increase extracellular  $K^+$  concentrations (Friedli, 1978; Galvan et al., 1979). Each spike is normally associated with a sharp transient rise in extracellular  $K^+$  concentration, which then rapidly falls and transiently undershoots before returning to the normal level (Galvan et al., 1979); ouabain slows the decline in  $K^+$  concentration after the spike and eliminates the undershoot. Continuous stimulation at a frequency of 6 Hz produces a sustained increase in extracellular  $K^+$  concentration (Galvan et al., 1979). It is likely that the increased extracellular  $K^+$  concentration and, almost certainly, increased intracellular  $Na^+$  concentration activate the  $Na^+$ ,  $K^+$ -ATPase, which in turn leads to the increased glucose utilization.

#### *Pharmacological Applications*

The ability of the deoxyglucose method to map the entire brain for localized regions of altered functional activity on the basis of changes in energy metabolism offers a potent tool to identify the neural sites of action of agents with neuropharmacological and psychopharmacological actions. It does not, however, discriminate between the direct and indirect effects of the drug. An entire pathway

may be activated even though the direct action of the drug may be exerted only at the origin of the pathway. This is of advantage for relating behavioral effects to central actions, but it is a disadvantage if the goal is to identify the primary site of action of the drug. To discriminate between direct and indirect actions of a drug the [ $^{14}C$ ]deoxyglucose method must be combined with selectively placed lesions in the CNS that interrupt afferent pathways to the structure in question. If the metabolic effect of the drug then remains, then it is due to direct action; if lost, the effect is likely to be indirect and mediated via the interrupted pathway. Nevertheless, the method has proved to be useful in a number of pharmacological studies.

**Effects of  $\gamma$ -butyrolactone.**  $\gamma$ -Hydroxybutyrate and  $\gamma$ -butyrolactone, which is hydrolyzed to  $\gamma$ -hydroxybutyrate in plasma, produce trance-like behavioral states associated with marked suppression of electroencephalographic activity (Roth and Giarman, 1966). These effects are reversible, and these drugs have been used clinically as anesthetic adjuvants. There is evidence that these agents lower neuronal activity in the nigrostriatal pathway and may act by inhibition of dopaminergic synapses (Roth, 1976). Studies in rats with the [ $^{14}C$ ]deoxyglucose technique have demonstrated that  $\gamma$ -

butyrolactone produces profound dose-dependent reductions of glucose utilization throughout the brain (Wolfson et al., 1977). At the highest doses studied, 600 mg/kg of body weight, glucose utilization was reduced by approximately 75% in gray matter and 33% in white matter, but there was no obvious further specificity with respect to the local cerebral structures affected. The reversibility of the effects and the magnitude and diffuseness of the depression of cerebral metabolic rate suggests that this drug might be considered as a chemical substitute for hypothermia in conditions in which profound reversible reduction of cerebral metabolism is desired.

**Effects of D-lysergic acid diethylamide.** The effects of the potent psychotomimetic agent, D-lysergic acid diethylamide, have been examined in the rat (Shinohara et al., 1976). In doses of 12.5–125  $\mu\text{g}/\text{kg}$ , it caused dose-dependent reductions in glucose utilization in a number of cerebral structures. With increasing dosage more structures were affected and to a greater degree. There was no pattern in the distribution of the effects, at least none discernible at the present level of resolution, that might contribute to the understanding of the drug's psychotomimetic actions.

**Effects of morphine addiction and withdrawal.** Acute morphine administration depresses glucose utilization in many areas of the brain, but the specific effects of morphine could not be distinguished from those of the hypercapnia produced by the associated respiratory depression (Sakurada et al., 1976). In contrast, morphine addiction, produced within 24 hours by a single subcutaneous injection of 150 mg/kg of morphine base in an oil emulsion, reduces glucose utilization in a large number of gray structures in the absence of changes in arterial  $\text{PCO}_2$ . White matter appears to be unaffected. Naloxone (1 mg/kg, s.c.) reduces glucose utilization in a number of structures when administered to normal rats, but when given to the morphine-addicted animals produces an acute withdrawal syndrome and reverses the reductions of glucose utilization in several structures, most strikingly in the habenula (Sakurada et al., 1976).

**Pharmacological studies of dopaminergic systems.** The most extensive applications of the deoxyglucose method to pharmacology have been in studies of dopaminergic systems. Ascending dopaminergic pathways appear to have a potent influence on glucose utilization in the forebrain of rats. Electrolytic lesions placed unilaterally in the

lateral hypothalamus or pars compacta of the substantia nigra caused marked ipsilateral reductions of glucose metabolism in numerous forebrain structures rostral to the lesion, particularly the frontal cerebral cortex, caudate-putamen, and parts of the thalamus (Schwartz et al., 1976; Schwartz, 1978). Similar lesions in the locus coeruleus had no such effects.

Enhancement of dopaminergic synaptic activity by administration of the agonist of dopamine, apomorphine (Brown and Wolfson, 1978), or of amphetamine (Wechsler et al., 1979), which stimulates release of dopamine at the synapse, produces marked increases in glucose consumption in some of the components of the extrapyramidal system known or suspected to contain dopamine-receptive cells. With both drugs, the greatest increases noted were in the zona reticulata of the substantia nigra and the subthalamic nucleus. Surprisingly, none of the components of the dopaminergic mesolimbic system appeared to be affected.

The studies with amphetamine (Wechsler et al., 1979) were carried out with the fully quantitative [ $^{14}\text{C}$ ]deoxyglucose method. The results in Table 5 illustrate the comprehensiveness with which this method surveys the entire brain for sites of altered activity due to actions of the drug. It also allows for quantitative comparison of the relative potencies of related drugs. For example, in Table 5, the comparative effects of *d*-amphetamine and the less potent dopaminergic agent, *l*-amphetamine, are compared; the quantitative results clearly reveal that the effects of *l*-amphetamine on local cerebral glucose utilization are more limited in distribution and of lesser magnitude than those of *d*-amphetamine. Indeed, in similar quantitative studies with apomorphine, McCulloch et al. (1979, 1980a) have been able to generate complete dose-response curves for the effects of the drug on the rates of glucose utilization in various components of dopaminergic system. They have also demonstrated metabolically the development of supersensitivity to apomorphine in rats maintained chronically on the dopamine-antagonist, haloperidol (J. McCulloch, H. E. Savaki, A. Pert, W. Bunney, and L. Sokoloff, unpublished observations). In the course of these studies with apomorphine, McCulloch et al. (1980b) obtained evidence of a retinal dopaminergic system that projects specifically to the superficial layer of the superior colliculus in the rat. Apomorphine administration activated metabolism in the superficial layer of the superior colliculus, as well as in other

TABLE 5. Effects of *d*-amphetamine and *l*-amphetamine on local cerebral glucose utilization in the conscious rat<sup>a</sup>

Structure	Local cerebral glucose utilization ( $\mu$ moles/100 g/min)		
	Control	<i>d</i> -Amphetamine	<i>l</i> -Amphetamine
<u>Gray Matter</u>			
Visual cortex	102 $\pm$ 8	135 $\pm$ 11 <sup>a</sup>	105 $\pm$ 8
Auditory cortex	160 $\pm$ 11	162 $\pm$ 6	141 $\pm$ 6
Parietal cortex	109 $\pm$ 9	125 $\pm$ 10	116 $\pm$ 4
Sensorimotor cortex	118 $\pm$ 8	139 $\pm$ 9	111 $\pm$ 4
Olfactory cortex	100 $\pm$ 6	93 $\pm$ 5	94 $\pm$ 3
Frontal cortex	109 $\pm$ 10	130 $\pm$ 8	105 $\pm$ 4
Prefrontal cortex	146 $\pm$ 10	166 $\pm$ 7	154 $\pm$ 4
Thalamus			
Lateral Nucleus	97 $\pm$ 5	114 $\pm$ 8	117 $\pm$ 6
Ventral nucleus	85 $\pm$ 7	108 $\pm$ 6 <sup>a</sup>	96 $\pm$ 4
Habenula	118 $\pm$ 10	71 $\pm$ 5 <sup>b</sup>	82 $\pm$ 2 <sup>b</sup>
Dorsomedial nucleus	92 $\pm$ 6	111 $\pm$ 8	106 $\pm$ 6
Medial geniculate	116 $\pm$ 5	119 $\pm$ 4	116 $\pm$ 4
Lateral geniculate	79 $\pm$ 5	88 $\pm$ 5	84 $\pm$ 4
Hypothalamus	54 $\pm$ 5	56 $\pm$ 3	52 $\pm$ 3
Suprachiasmatic nucleus	94 $\pm$ 4	75 $\pm$ 4 <sup>b</sup>	67 $\pm$ 1 <sup>b</sup>
Mamillary body	117 $\pm$ 8	134 $\pm$ 5	142 $\pm$ 5 <sup>a</sup>
Lateral olfactory nucleus <sup>d</sup>	92 $\pm$ 6	95 $\pm$ 5	99 $\pm$ 6
A <sub>13</sub>	71 $\pm$ 4	91 $\pm$ 4 <sup>b</sup>	81 $\pm$ 4
Hippocampus			
Ammon's horn	79 $\pm$ 5	73 $\pm$ 2	81 $\pm$ 6
Dentate gyrus	60 $\pm$ 4	55 $\pm$ 3	67 $\pm$ 7
Amygdala	46 $\pm$ 3	46 $\pm$ 3	44 $\pm$ 2
Septal nucleus	56 $\pm$ 3	55 $\pm$ 2	54 $\pm$ 3
Caudate nucleus	109 $\pm$ 5	132 $\pm$ 8 <sup>a</sup>	127 $\pm$ 3 <sup>a</sup>
Nucleus accumbens	76 $\pm$ 5	80 $\pm$ 3	78 $\pm$ 3
Globus pallidus	53 $\pm$ 3	64 $\pm$ 2 <sup>a</sup>	65 $\pm$ 3 <sup>a</sup>
Subthalamic nucleus	89 $\pm$ 6	149 $\pm$ 10 <sup>b</sup>	107 $\pm$ 2
Substantia nigra			
Zona reticulata	58 $\pm$ 2	105 $\pm$ 4 <sup>b</sup>	72 $\pm$ 4
Zona compacta	65 $\pm$ 4	88 $\pm$ 6 <sup>b</sup>	72 $\pm$ 3
Red nucleus	76 $\pm$ 5	94 $\pm$ 5 <sup>a</sup>	86 $\pm$ 2
Vestibular nucleus	121 $\pm$ 11	137 $\pm$ 5	130 $\pm$ 4
Cochlear nucleus	139 $\pm$ 6	126 $\pm$ 1	141 $\pm$ 5
Superior olivary nucleus	144 $\pm$ 4	143 $\pm$ 4	147 $\pm$ 6
Lateral lemniscus	107 $\pm$ 3	96 $\pm$ 5	98 $\pm$ 3
Inferior colliculus	193 $\pm$ 10	169 $\pm$ 5	150 $\pm$ 8 <sup>b</sup>
Dorsal tegmental nucleus	109 $\pm$ 5	112 $\pm$ 7	122 $\pm$ 6
Superior colliculus	80 $\pm$ 5	89 $\pm$ 3	91 $\pm$ 3
Pontine gray	58 $\pm$ 4	65 $\pm$ 3	60 $\pm$ 1
Cerebellar flocculus	124 $\pm$ 10	146 $\pm$ 15	153 $\pm$ 10
Cerebellar hemispheres	55 $\pm$ 3	68 $\pm$ 6	64 $\pm$ 2
Cerebellar nuclei	102 $\pm$ 4	105 $\pm$ 8	110 $\pm$ 3
<u>White Matter</u>			
Corpus callosum	23 $\pm$ 3	24 $\pm$ 2	23 $\pm$ 1
Genu of corpus callosum	29 $\pm$ 2	30 $\pm$ 2	26 $\pm$ 2
Internal capsule	21 $\pm$ 1	24 $\pm$ 2	19 $\pm$ 2
Cerebellar white	28 $\pm$ 1	31 $\pm$ 2	31 $\pm$ 2

<sup>a</sup> All values are the means  $\pm$  standard error of the mean for 5 animals.

<sup>b</sup> Significant difference from the control at the  $p < 0.05$  level.

<sup>c</sup> Significant difference from the control at the  $p < 0.01$  level.

<sup>d</sup> It was not possible to correlate precisely this area on autoradiographs with a specific structure in the rat brain. It is, however, most likely the lateral olfactory nucleus.

From Wechsler et al., 1979.

structures, but the effect in the superficial layer was prevented by prior enucleation (Fig. 9). Miyaoka (unpublished observations) subsequently observed that intraocular administration of minute amounts of apomorphine caused increased glucose utilization only in the superficial layer of the superior colliculus of the contralateral side.

**Effects of  $\alpha$ - and  $\beta$ -adrenergic blocking agents.** Savaki et al. (1978) have studied the effects of the

$\alpha$ -adrenergic-blocking agent, phentolamine, and the  $\beta$ -adrenergic-blocking agent, propranolol. Both drugs produced widespread dose-dependent depressions of glucose utilization throughout the brain, but exhibit particularly striking and opposite effects in the complete auditory pathway from the cochlear nucleus to the auditory cortex. Propranolol markedly depressed and phentolamine markedly enhanced glucose utilization in this pathway. The

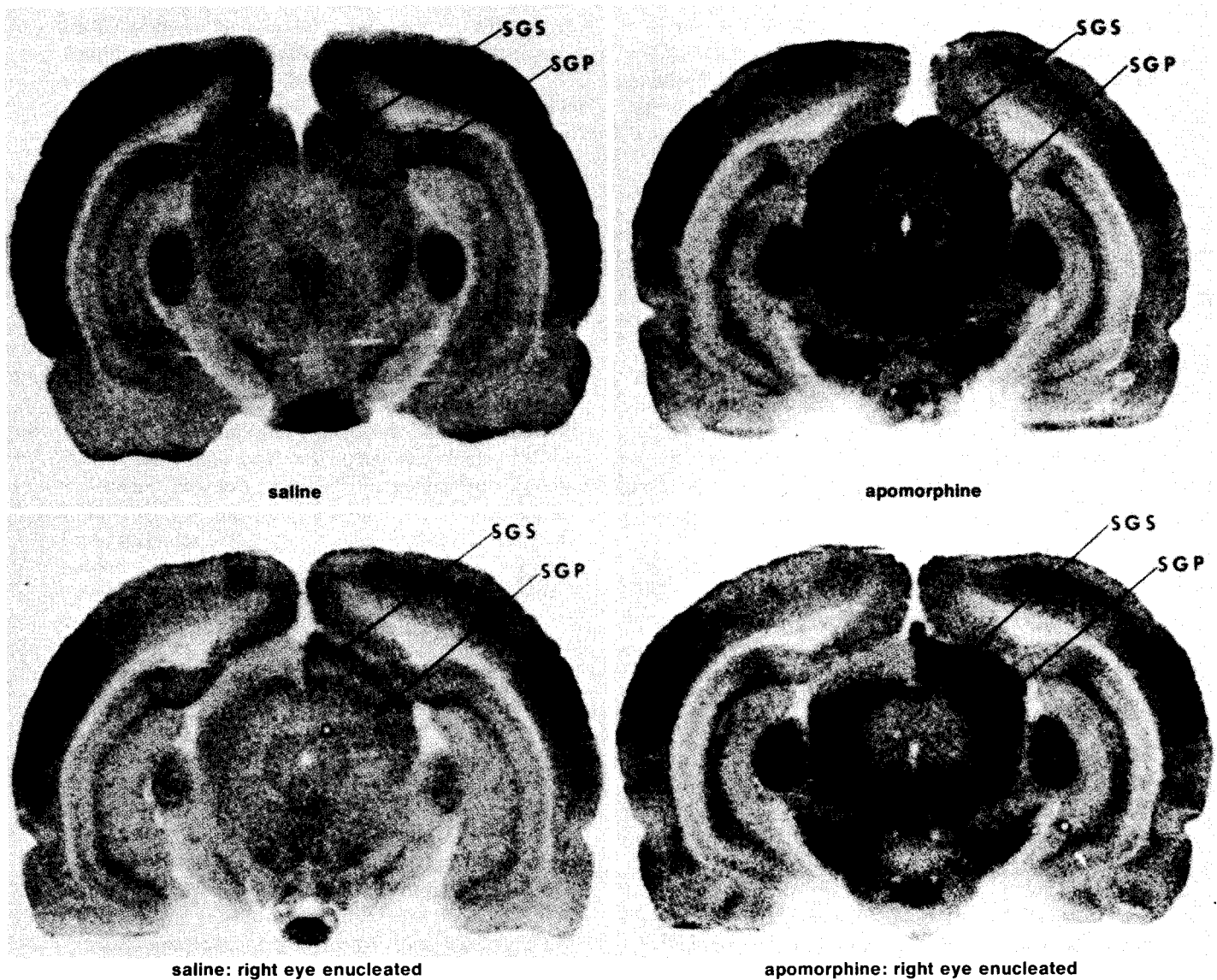


**FIG. 9.** Representative autoradiographs at the level of superior colliculus in dark-adapted rats studied in the dark. **Upper left:** Saline, intact visual system. **Upper right:** Apomorphine (1.5 mg/kg), intact visual system. Note bilaterally increased optical density (that is, elevated glucose utilization) in both superficial and deep laminae of the superior colliculus. **Lower left:** Saline, right eye enucleated. Asymmetrical optical density with reduction on contralateral side is apparent within the superficial layer, whereas in the deeper layer the optical density remains symmetrical. **Lower right:** Apomorphine (1.5 mg/kg), right eye enucleated. Note increased optical density bilaterally in the deeper layer but only in the right or ipsilateral superficial layer of the superior colliculus. *Abbreviations:* SGS, stratum griseum superficiale; SGP, stratum griseum profundum. (From McCulloch et al., 1980b.)

functional significance of these effects is unknown, but they seem to correlate with corresponding effects on the electrophysiological responsiveness of this sensory system. Propranolol depresses and phentolamine enhances the amplitude of all components of evoked auditory responses (T. Furlow and J. Hallenbeck, personal communication).

#### *Pathophysiological Applications*

The application of the deoxyglucose method to the study of pathological states has been limited because of uncertainties about the values for the lumped and rate constants to be used. There are, however, pathophysiological states in which there is no structural damage to the tissue, and the standard values of the constants can be used. Several of these conditions have been and are continuing to be studied by the [ $^{14}\text{C}$ ]deoxyglucose technique, both qualitatively and quantitatively.

**Convulsive states.** The local injection of penicillin into the motor cortex produces focal seizures manifested in specific regions of the body contralaterally. The [ $^{14}\text{C}$ ]deoxyglucose method has been used to map the spread of seizure activity within the brain and to identify the structures with altered functional activity during the seizure. The partial results of one such experiment in the monkey are illustrated in Fig. 3. Discrete regions of markedly increased glucose utilization, sometimes as much as 200%, are observed ipsilaterally in the motor cortex, basal ganglia, particularly the globus pallidus, thalamic nuclei, and contralaterally in the cerebellar cortex (Kennedy et al., 1975). Kato et al. (1980), Caveness et al. (1980), Hosokawa et al. (1980), and Caveness (1980) have carried out the most extensive studies of the propagation of the seizure activity in newborn and pubescent monkeys. The results indicate that the brain of the newborn monkey exhibits similar increases of glucose utilization in specific structures, but the pattern of distribution of the effects is less well-defined than in the pubescent monkeys. Collins et al. (1976) have carried out similar studies in the rat with similar results but also obtained evidence based on local stimulation of glucose utilization for a "mirror focus" in the motor cortex contralateral to the side with the penicillin-induced epileptogenic focus.

Engel et al. (1978) have used the [ $^{14}\text{C}$ ]deoxyglucose method to study seizures kindled in rats by daily electroconvulsive shocks. After a period of such treatment, the animals exhibit spontaneous

seizures. Their results show marked increases in the limbic system, particularly the amygdala. The daily administration of the local anesthetic, lidocaine, kindles similar seizures in rats; Post et al. (1979) have obtained similar results in such seizures, with particularly pronounced increases in glucose utilization in the amygdala, hippocampus, and the enterorhinal cortex.

**Spreading cortical depression.** Shinohara et al. (1979) studied the effects of local applications of KCl on the dura overlying the parietal cortex of conscious rats or directly on the pial surface of the parietal cortex of anesthetized rats in order to determine if  $\text{K}^+$  stimulates cerebral energy metabolism *in vivo* as it is well-known to do *in vitro*. The results demonstrate a marked increase in cerebral cortical glucose utilization in response to the application of KCl; NaCl has no such effect (Fig. 10). Such application of KCl, however, also produces the phenomenon of spreading cortical depression. This condition is characterized by a spread of transient intense neuronal activity followed by membrane depolarization, electrical depression, and a negative shift in the cortical DC potential in all directions from the site of initiation at a rate of 2–5 mm/min. The depressed cortex also exhibits a number of chemical changes, including an increase in extracellular  $\text{K}^+$ , lost presumably from the cells. At the same time when the cortical glucose utilization is increased, most subcortical structures that are functionally connected to the depressed cortex exhibit decreased rates of glucose utilization. During recovery from the spreading cortical depression, the glucose utilization in the cortex is still increased, but is distributed in columns oriented perpendicularly through the cortex. This columnar arrangement may reflect the columnar functional and morphological arrangement of the cerebral cortex. It is likely that the increased glucose utilization in the cortex during spreading cortical depression is the consequence of the increased extracellular  $\text{K}^+$  and activation of the  $\text{Na}^+$ ,  $\text{K}^+$ -ATPase.

**Opening of blood-brain barrier.** Unilateral opening of the blood-brain barrier in rats by unilateral carotid injection with a hyperosmotic mannitol solution leads to widely distributed discrete regions of intensely increased glucose utilization in the ipsilateral hemisphere (Pappius et al., 1979). These focal regions of hypermetabolism may reflect local regions of seizure activity. The prior administration of diazepam prevents the appearance of these areas

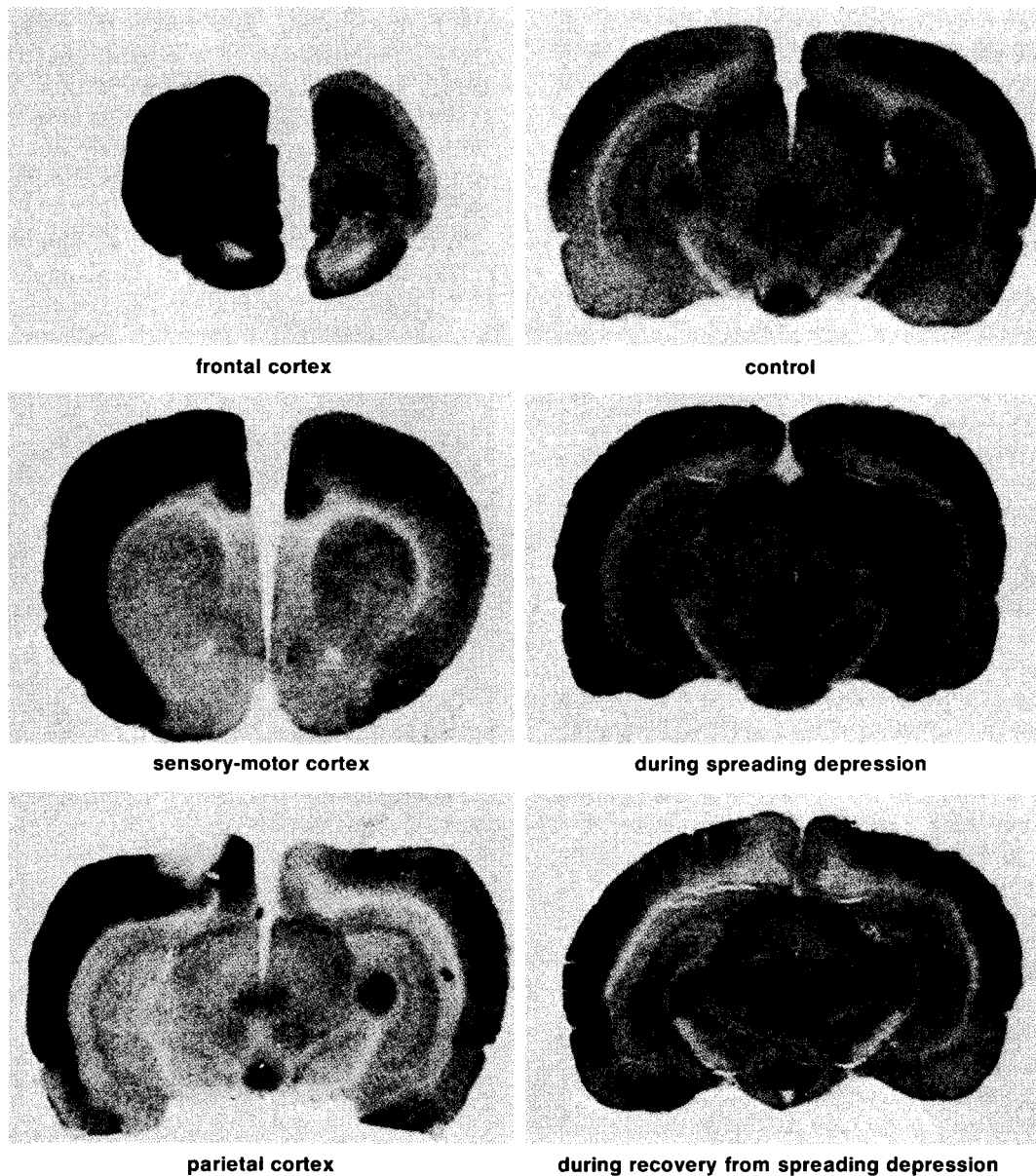


**FIG. 10.** Autoradiographs of sections of rat brains during spreading cortical depression and during recovery. The autoradiographs are pictorial representations of the relative rates of glucose utilization in various parts of the brain—the greater the density, the greater the rate of glucose utilization. The left sides of the brain are represented by the left hemispheres in the autoradiographs. In all the experiments illustrated, the control hemisphere was treated the same as the experimental side except that equivalent concentrations of NaCl rather than KCl were used. The NaCl did not lead to any detectable differences from hemispheres over which the skull was left intact and no NaCl was applied. **Left:** Autoradiographs of sections of brain at different levels of cerebral cortex from a conscious rat during spreading cortical depression induced on the left side by application of 5 M KCl to the intact dura overlying the left parietal cortex. The spreading depression was sustained by repeated applications of the KCl at 15- to 20-minute intervals throughout the experimental period. **Right:** Autoradiographs from sections of brain at the level of the parietal cortex from 3 animals under barbiturate anesthesia. The top section is from a normal anesthetized animal; the middle section is from an animal during unilateral spreading cortical depression induced and sustained by repeated applications of 80 mM KCl in artificial cerebrospinal fluid directly on the surface of the left parieto-occipital cortex. At the bottom is a comparable section from an animal studied immediately after the return of cortical DC potential to normal after a single wave of spreading depression induced by a single application of 80 mM KCl to the parieto-occipital cortex of the left side. (From Shinohara et al., 1979.)

of increased metabolism in most cases (Pappius et al., 1979), and electroencephalographic recordings under similar experimental conditions reveal evidence of seizure activity (C. Fieschi, personal communication).

**Hypoxemia.** Pulsinelli and Duffy (1979) have studied the effects of controlled hypoxemia on local cerebral glucose utilization by means of the qualitative [ $^{14}\text{C}$ ]deoxyglucose method. Hypoxemia was achieved by artificial ventilation of the animals with a mixture of  $\text{N}_2$ ,  $\text{N}_2\text{O}$ , and  $\text{O}_2$  adjusted to maintain the arterial  $\text{Po}_2$  between 28 and 32 mm Hg. All the animals had had one common carotid artery ligated to limit the increase in cerebral blood flow and the amount of  $\text{O}_2$  delivered to the brain. Their autoradiographs provide striking evidence of marked and disparate changes in glucose utilization in the various structural components of the brain. The hemisphere ipsilateral to the carotid ligation was, not unexpectedly, more severely affected. The most striking effects were markedly higher increases in glucose utilization in white matter than in gray matter, presumably due to the Pasteur effect, and the appearance of transverse cortical columns of high activity alternating with columns of low activity. By studies with black plastic microspheres, they were able to show that the cortical columns were anatomically related to penetrating cortical arteries, with the columns of high metabolic activity lying between the arteries.

Miyaoka et al. (1979b) have also studied the effects of moderate hypoxemia in normal, spontaneously breathing conscious rats without carotid ligation. The hypoxemia was produced by lowering the  $\text{O}_2$  in the inspired air to approximately 7%. Although this procedure reduced arterial  $\text{Po}_2$  to approximately 30 mm Hg, the cerebral hypoxia was probably less than in the studies of Pulsinelli and Duffy (1979) because of the intact cerebral circulation. The animals remained fully conscious under these experimental conditions, although they appeared subdued and less active. The quantitative [ $^{14}\text{C}$ ]deoxyglucose method was employed, and rates of glucose utilization were determined. The results revealed many similarities to those of Pulsinelli and Duffy (1979). There was a complete redistribution of the local rates of glucose utilization from the normal pattern. Metabolism in white matter was markedly increased. Many areas showed decreased rates of metabolism. Columns were seen in the cerebral cortex, and the caudate nucleus exhibited a strange lace-like heterogeneity quite distinct from

its normal homogeneity. Despite the widespread changes, however, overall average glucose utilization remained unchanged. These results are of relevance to the studies by Kety and Schmidt (1948b), who found in man that the breathing of 10%  $\text{O}_2$  produced a wide variety of mental symptoms without altering the average  $\text{O}_2$  consumption of the brain as a whole. The mental symptoms were probably the result of metabolic and functional changes in specific regions of the brain detectable only by methods like the deoxyglucose method that measure metabolic rate in the structural components of the brain.

**Normal aging.** Although, strictly speaking, aging is not a pathophysiological condition, many of its behavioral consequences are directly attributable to decrements in functions of the central nervous system (Birren et al., 1963). Normal human aging has been found to be associated with a decrease in average glucose utilization of the brain as a whole (Sokoloff, 1966). Smith et al. (1980) have employed the quantitative [ $^{14}\text{C}$ ]deoxyglucose method to study normal aging in Sprague-Dawley rats between 5–6 and 36 months of age. Their results show widespread but not homogeneous reductions of local cerebral glucose utilization with age. The sensory systems, particularly auditory and visual, are particularly severely affected. The caudate nucleus is metabolically depressed, and preliminary experiments indicate that it loses responsivity to dopamine agonists, such as apomorphine, with age (C. Smith and J. McCulloch, unpublished observations). A striking effect was the loss of metabolically active neuropil in the cerebral cortex; Layer IV is markedly decreased in metabolic activity and extent. Some of these changes may be related to specific functional disabilities that develop in old age.

### Microscopic Resolution

The resolution of the present [ $^{14}\text{C}$ ]deoxyglucose method is at best approximately 100  $\mu\text{m}$ . The use of [ $^3\text{H}$ ]DG does not greatly improve the resolution when the standard autoradiographic procedure is used. The limiting factor is the diffusion and migration of the water-soluble labeled compound in the tissue during the freezing of the brain and the cutting of the brain sections. Des Rosiers and Descarries (1978) have been working to extend the resolution of the method to the light and electron microscopic levels. They use [ $^3\text{H}$ ]DG and dipping emulsion

techniques, and they have reported that fixation, postfixation, dehydration, and embedding of the brain by perfusion *in situ* results in negligible loss or migration of the label in the tissue. They can localize grain counts over individual cells or portions of them. Although the method is at present only qualitative, it is likely that it can eventually be adopted for quantitative use. An alternative promising approach to microscopic resolution is the use of freeze-substitution techniques (Ornberg et al., 1979; Sejnowski et al., 1980).

#### [<sup>18</sup>F]Fluorodeoxyglucose Technique

Because the deoxyglucose method requires the measurement of local concentrations of radioactivity in the individual components of the brain, it cannot be applied as originally designed to man. Recent developments in computerized emission tomography, however, have made it possible to measure local concentrations of labeled compounds *in vivo* in man. Emission tomography requires the use of  $\gamma$ -radiation, preferably annihilation  $\gamma$ -rays derived from positron emission. A positron-emitting derivative of deoxyglucose, 2-[<sup>18</sup>F]fluoro-2-deoxy-D-glucose has been synthesized and found to retain the necessary biochemical properties of DG (Reivich et al., 1979). The method has, therefore, been adapted for use in man with [<sup>18</sup>F]fluorodeoxyglucose and positron-emission tomography (Phelps et al., 1979; Reivich et al., 1979). The resolution of the method is still relatively limited, approximately 1 cm, but it is already proving to be useful in studies of the human visual system (Phelps et al., 1981) and of clinical conditions, such as focal epilepsy (Kuhl et al., 1979, 1980). This technique is of immense potential usefulness for studies of human local cerebral energy metabolism in normal states and in neurological and psychiatric disorders.

#### Relationship Between Local Energy Metabolism and Local Blood Flow in the Brain

The concept that the regulation of the cerebral circulation is at least in part mediated by the products of cerebral metabolism and that cerebral blood flow is adjusted to local cerebral metabolism and functional activity is almost a century old. In a classic paper published in 1890, Roy and Sherrington (1890) stated "the chemical products of cerebral

metabolism contained in the lymph which bathes the walls of the arterioles of the brain can cause variations of the calibre of the cerebral vessels . . . in this re-action the brain possesses an intrinsic mechanism by which its vascular supply can be varied locally in correspondence with local variations of functional activity." The validity of this hypothesis has been generally assumed, and it has been the basis of many of our current ideas about the regulation of the cerebral circulation. Direct experimental evidence in support of it, however, has awaited the development of methods for the measurement of blood flow and energy metabolism in discrete structural components of the brain exhibiting alterations in functional activity.

The availability of the [<sup>14</sup>C]deoxyglucose method for measuring glucose utilization and the [<sup>14</sup>C]-iodoantipyrine method (Sakurada et al., 1978) for measuring blood flow in individual discrete structural and functional components of the brain has made it possible to examine directly the relationship between them. The results demonstrate that they are indeed closely related (Des Rosiers et al., 1974). In normal conscious rat the coefficient of correlation between the rates of glucose utilization and blood flow in the various cerebral structures is equal to 0.95 ( $p < 0.001$ ) (Fig. 11A). Thiopental anesthesia reduces the rates of both metabolism and blood flow in almost all the structures, but the correlation, though reduced, still remains quite close ( $r = 0.80$ ,  $p < 0.001$ ) (Fig. 11B). These results confirm that the individual cerebral structures are normally perfused more or less in proportion to their metabolic demands.

Not only do the rates of blood flow in the various structural components of the brain normally parallel the local rates of glucose consumption, but local blood flow is generally altered, just as local energy metabolism is, in response to changes in local functional activity. Local blood flow is measured with an autoradiographic technique like that of the [<sup>14</sup>C]-deoxyglucose technique that demonstrates the relative rates of blood flow in the various cerebral structures. These autoradiographs demonstrate that the same structures that exhibit changes in glucose utilization also exhibit comparable changes in blood flow in altered physiological states. For example, retinal stimulation with a photoflash produces increased blood flow in discrete regions of the visual cortex, lateral geniculate body, and superior colliculus of the conscious cat (Sokoloff, 1961). Unilateral enucleation in the rat reduces blood flow

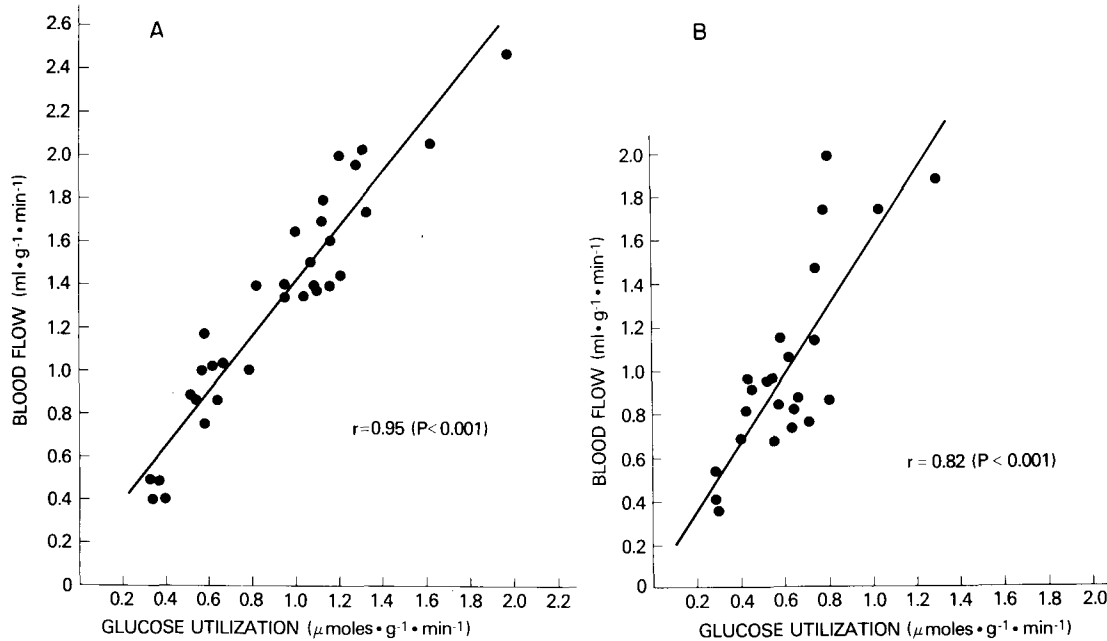


**FIG. 11.** Correlation between local cerebral blood flow, measured with the  $^{14}\text{C}$ jodoantipyrine technique (Sakurada et al., 1978) and local cerebral utilization of glucose measured with the  $^{14}\text{C}$ deoxyglucose technique (Sokoloff et al., 1977). Each point represents a different structure in the brain. **A:** Normal conscious rat. Each point represents the mean local glucose utilization obtained from 10 rats and the mean local blood flow obtained from 6 rats. **B:** Animals under thiopental anesthesia. Each point represents the mean values of local glucose utilization and blood flow obtained from 8 animals and 6 animals, respectively. (From Sokoloff, 1978a.)

and glucose utilization contralaterally in these structures; indeed, the autoradiographs obtained with  $^{14}\text{C}$ jodoantipyrine are then almost indistinguishable from those obtained with  $^{14}\text{C}$ -deoxyglucose. Focal seizures produced by the application of penicillin to the motor cortex in the monkey result in local increases in blood flow in the same structures that exhibit increased glucose consumption (Fig. 3) (Caveness et al., 1975).

It is clear from the results of the studies of local cerebral blood flow and glucose utilization that energy metabolism and functional activity are closely coupled in the nervous system and that local blood flow is distributed and adjusted in the cerebral tissues to local metabolic demand and thereby to local functional activity. The results fully confirm this hypothesis of Roy and Sherrington (1890), but the mechanisms responsible for the close coupling of these vital functions remain unknown.

### Summary

The deoxyglucose method provides the means to determine quantitatively the rates of glucose utilization simultaneously in all structural and func-

tional components of the central nervous system and to display them pictorially superimposed on the anatomical structures in which they occur. Because of the close relationship between local functional activity and energy metabolism, the method makes it possible to identify all structures with increased or decreased functional activity in various physiological, pharmacological, and pathophysiological states. The images provided by the method do resemble histological sections of nervous tissue, and the method is, therefore, sometimes misconstrued to be a neuroanatomical method and contrasted with physiological methods, such as electrophysiological recording. This classification obscures the most significant and unique feature of the method. The images are not of structure but of a dynamic biochemical process, glucose utilization, which is as physiological as electrical activity. In most situations changes in functional activity result in changes in energy metabolism, and the images can be used to visualize and identify the sites of altered activity. The images are, therefore, analogous to infrared maps; they record quantitatively the rates of a kinetic process and display them pictorially exactly where they exist. The fact that

they depict the anatomical structures is fortuitous; it indicates that the rates of glucose utilization are distributed according to structure, and specific functions in the nervous system are associated with specific anatomical structures. The deoxyglucose method represents, therefore, in a real sense, a new type of encephalography, metabolic encephalography. At the very least, it should serve as a valuable supplement to more conventional types, such as electroencephalography. Because, however, it provides a new means to examine another aspect of function simultaneously in all parts of the brain, it is hoped that it and its derivative, the [ $^{18}\text{F}$ ]fluoro-deoxyglucose technique, will open new roads to the understanding of how the brain works in health and disease.

### Acknowledgment

The author wishes to express his appreciation to Mrs. Ruth Bower for her excellent editorial and bibliographic assistance.

### References

- Bachelard HS (1971) Specificity and kinetic properties of monosaccharide uptake into guinea pig cerebral cortex *in vitro*. *J Neurochem* 18:213–222.
- Batipps M, Miyaoka M, Shinohara M, Sokoloff L, and Kennedy C (1981) Comparative rates of local cerebral glucose utilization in the visual system of conscious albino and pigmented rats. *Neurology* 31:58–62.
- Bidder TG (1968) Hexose translocation across the blood-brain interface: Configurational aspects. *J Neurochem* 15:867–874.
- Birren JE, Butler RN, Greenhouse SW, Sokoloff L, and Yarrow MR (eds) (1963) *Human Aging: A Biological and Behavioral Study*. Public Health Service Publication No. 986. Washington DC, U.S. Government Printing Office.
- Brown L and Wolfson L (1978) Apomorphine increases glucose utilization in the substantia nigra, subthalamic nucleus, and corpus striatum of the rat. *Brain Res* 148:188–193.
- Caveness WF (1969) Ontogeny of focal seizures. In: *Basic Mechanisms of the Epilepsies* (Jasper HH, Ward AA, and Pope A, eds), Boston, Little, Brown, pp. 517–534.
- Caveness WF (1980) Appendix: Tables of local cerebral glucose utilization in various experimental preparations. *Ann Neurol* 7:230–237.
- Caveness WF, Ueno H, and Kemper TL (1975) Subcortical factors in experimental Jacksonian seizures. In *Proceedings of the 7th International Congress on Neuropathology*, Vol. 2 (Kornyei S, Tariska S, and Gosztanyi G, eds) Excerpta Medica, Amsterdam, pp 29–34.
- Caveness WF, Kato M, Malamut BL, Hosokawa S, Wakisaka S, and O'Neill RR (1980) Propagation of focal motor seizures in the pubescent monkey. *Ann Neurol* 7:213–221.
- Collins RC, Kennedy C, Sokoloff L, and Plum F (1976) Metabolic anatomy of focal motor seizures. *Arch Neurol* 33:536–542.
- Des Rosiers MH and Descarries L (1978) Adaptation de la méthode au désoxyglucose à l'échelle cellulaire: Préparation histologique du système nerveux central en vue de la radioautographie à haute résolution. *CR Acad Sci, Ser D* 287:153–156.
- Des Rosiers MH, Kennedy C, Patlak CS, Pettigrew KD, Sokoloff L, and Reivich M (1974) Relationship between local cerebral blood flow and glucose utilization in the rat. *Neurology* 24:389.
- Des Rosiers MH, Sakurada O, Jehle J, Shinohara M, Kennedy C, and Sokoloff L (1978) Functional plasticity in the immature striate cortex of the monkey shown by the [ $^{14}\text{C}$ ]deoxyglucose method. *Science* 200:447–449.
- Duffy TE, Cavazzuit M, Gregoire NM, Cruz NF, Kennedy C, and Sokoloff L (1979) Regional cerebral glucose metabolism in newborn beagle dogs. *Trans Am Soc Neurochem* 10:171
- Durham D and Woolsey TA (1977) Barrels and columnar cortical organization: Evidence from 2-deoxyglucose (2-DG) experiments. *Brain Res* 137:169–174.
- Eklöf B, Lassen NA, Nilsson L, Norberg K, and Siesjö BK (1973) Blood flow and metabolic rate for oxygen in the cerebral cortex of the rat. *Acta Physiol Scand* 88:587–589.
- Engel J Jr, Wolfson L, and Brown L (1978) Anatomical correlates of electrical and behavioral events related to amygdaloid kindling. *Ann Neurol* 3:538–544.
- Freygang WH Jr and Sokoloff L (1958) Quantitative measurement of regional circulation in the central nervous system by the use of radioactive inert gas. *Adv Biol Med Phys* 6:263–279.
- Friedli C (1978) Kinetics of changes in  $\text{pO}_2$  and extracellular potassium activity in stimulated rat sympathetic ganglia. *Adv Exp Med Biol* 94:747–754.
- Galvan M, Ten Bruggencate G, and Senekowitsch R (1979) The effects of neuronal stimulation and ouabain upon extracellular  $\text{K}^+$  and  $\text{Ca}^{2+}$  levels in rat isolated sympathetic ganglia. *Brain Res* 160:544–548.
- Gjedde A, Caronna JJ, Hindfelt B, and Plum F (1975) Whole-brain blood flow and oxygen metabolism in the rat during nitrous oxide anesthesia. *Am J Physiol* 229:113–118.
- Gooch C, Rasband W, and Sokoloff L (1980) Computerized densitometry and color coding of [ $^{14}\text{C}$ ]deoxyglucose autoradiographs. *Ann Neurol* 7:359–370.
- Hand PJ (1981) The 2-deoxyglucose method. In: *Methods in Contemporary Neuroanatomy: The Tracing of Central Nervous Pathways* (Heimer L, and Robards MJ, eds), New York, Plenum (in press).
- Hand PJ, Greenberg JH, Miselis RR, Weller WL, and Reivich M. (1978) A normal and altered cortical column: A quantitative and qualitative ( $^{14}\text{C}$ )-2 deoxyglucose (2DG) mapping study. *Neurosci Abstr* 4:553.
- Hers HG (1957) *Le Métabolisme du Fructose*. Brussels, Editions Arscia, p. 102.
- Horowicz P and Larrabee MG (1958) Glucose consumption and lactate production in a mammalian sympathetic ganglion at rest and in activity. *J Neurochem* 2:102–118.
- Hosokawa S, Iguchi T, Caveness WF, Kato M, O'Neill RR, Wakisaka S, and Malamut BL (1980) Effects of manipulation of the sensorimotor system on focal motor seizures in the monkey. *Ann Neurol* 7:222–229.
- Hubel DH and Wiesel TN (1968) Receptive fields and functional architecture of monkey striate cortex. *J Physiol (London)* 195:215–243.
- Hubel DH and Wiesel TN (1972) Laminar and columnar distribution of geniculo-cortical fibers in the Macaque monkey. *J Comp Neurol* 146:421–450.
- Hubel DH, Wiesel TN, and Stryker MP (1978) Anatomical demonstration of orientation columns in macaque monkey. *J. Comp. Neurol.* 177:361–380.
- Jarvis CD, Mishkin M, Shinohara M, Sakurada O, Miyaoka M, and Kennedy C (1978) Mapping the primate visual system with the [ $^{14}\text{C}$ ]2-deoxyglucose technique. *Neurosci Abstr* 4:632.

- Kato M, Malamut BL, Caveness WF, Hosokawa S, Wakisaka S, and O'Neill RR (1980) Local cerebral glucose utilization in newborn and pubescent monkeys during focal motor seizures. *Ann Neurol* 7:204-212.
- Kennedy C, Des Rosiers M, Jehle JW, Reivich M, Sharp F, and Sokoloff L (1975) Mapping of functional neural pathways by autoradiographic survey of local metabolic rate with [<sup>14</sup>C]deoxyglucose. *Science* 187:850-853.
- Kennedy C, Des Rosiers MH, Sakurada O, Shinohara M, Reivich M, Jehle JW, and Sokoloff L (1976) Metabolic mapping of the primary visual system of the monkey by means of the autoradiographic [<sup>14</sup>C]deoxyglucose technique. *Proc Natl Acad Sci USA* 73:4230-4234.
- Kennedy C, Sakurada O, Shinohara M, Jehle J, and Sokoloff L (1978) Local cerebral glucose utilization in the normal conscious macaque monkey. *Ann Neurol* 4:293-301.
- Kennedy C, Miyaoka M, Suda S, Macko K, Jarvis C, Mishkin M, and Sokoloff L (1980) Local metabolic responses in brain accompanying motor activity. *Trans Am Neurol Assoc* (in press).
- Kety SS (1950) Circulation and metabolism of the human brain in health and disease. *Am J Med* 8:205-217.
- Kety SS (1957) The general metabolism of the brain *in vivo*. In: *Metabolism of the Nervous System* (Richter D, ed). London, Pergamon Press, pp 221-237.
- Kety SS (1960) Measurement of local blood flow by the exchange of an inert, diffusible substance. *Methods Med Res* 8:228-236.
- Kety SS and Schmidt CF (1948a) The nitrous oxide method for the quantitative determination of cerebral blood flow in man: Theory, procedure, and normal values. *J Clin Invest* 27:476-483.
- Kety SS and Schmidt CF (1948b) Effects of altered arterial tensions of carbon dioxide and oxygen on cerebral blood flow and cerebral oxygen consumption of normal young men. *J Clin Invest* 27:484-492.
- Kuhl D, Engel J, Phelps M, and Selin C (1979) Patterns of local cerebral metabolism and perfusion in partial epilepsy by emission computed tomography of <sup>18</sup>F-fluorodeoxyglucose and <sup>13</sup>N-ammonia. *Acta Neurol Scand Suppl* 72 60:538-539.
- Kuhl DE, Engel J Jr, Phelps ME, and Selin C (1980) Epileptic patterns of local cerebral metabolism and perfusion in humans determined by emission computed tomography of <sup>18</sup>FDG and <sup>13</sup>NH<sub>3</sub>. *Ann Neurol* 8:348-360.
- Landau WM, Freygang WH Jr, Rowland LP, Sokoloff L, and Kety SS (1955) The local circulation of the living brain: values in the unanesthetized and anesthetized cat. *Trans Am Neurol Assoc* 80:125-129.
- Larrabee MG (1958) Oxygen consumption of excised sympathetic ganglia at rest and in activity. *J Neurochem* 2:81-101.
- Lashley KS (1934) The mechanism of vision. VII. The projection of the retina upon the primary optic centers of the rat. *J Comp Neurol* 59:341-373.
- Lassen NA (1959) Cerebral blood flow and oxygen consumption in man. *Physiol Rev* 39:183-238.
- Lassen NA and Munck O (1955) The cerebral blood flow in man determined by the use of radioactive krypton. *Acta Physiol Scand* 33:30-49.
- Mata M, Fink DJ, Gainer H, Smith CB, Davidsen L, Savaki H, Schwartz WJ, and Sokoloff L (1980) Activity-dependent energy metabolism in rat posterior pituitary reflects sodium pump activity. *J Neurochem* 34:213-215.
- McCulloch J, Savaki HE, McCulloch MC, and Sokoloff L (1979) Specific distribution of metabolism alterations in cerebral cortex following apomorphine administration. *Nature* 282:303-305.
- McCulloch J, Savaki HE and Sokoloff L (1980a) Influence of dopaminergic systems on the lateral habenular nucleus of the rat. *Brain Res* 194:117-124.
- McCulloch J, Savaki HE, McCulloch MC, and Sokoloff L (1980b) Retina-dependent activation by apomorphine of metabolic activity in the superficial layer of superior colliculus. *Science* 207:313-315.
- Miyaoka M, Shinohara M, Batipps M, Pettigrew KD, Kennedy C, and Sokoloff L (1979a) The relationship between the intensity of the stimulus and the metabolic response in the visual system of the rat. *Acta Neurol Scand Suppl* 72 60:16-17.
- Miyaoka M, Shinohara M, Kennedy C, and Sokoloff L (1979b) Alterations in local cerebral glucose utilization (LCGU) in rat brain during hypoxemia. *Trans Am Neurol Assoc* 104:151-154.
- Montero VM and Guillery RW (1968) Degeneration in the dorsal lateral geniculate nucleus of the rat following interruption of the retinal or cortical connections. *J Comp Neurol* 134:211-242.
- Oldendorf WH (1971) Brain uptake of radiolabeled amino acids, amines, and hexoses after arterial injection. *Am J Physiol* 221:1629-1638.
- Ornberg RL, Neale EA, Smith CB, Yarowsky P, and Bowers LM (1979) Radioautographic localization of glucose utilization by neurons in culture. *J Cell Biol Abstr* 83:CN142A.
- Pappius HM, Savaki HE, Fieschi C, Rapoport SI, and Sokoloff L (1979) Osmotic opening of the blood-brain barrier and local cerebral glucose utilization. *Ann Neurol* 5:211-219.
- Phelps ME, Huang SC, Hoffman EJ, Selin C, Sokoloff L, and Kuhl DE (1979) Tomographic measurement of local cerebral glucose metabolic rate in humans with (F-18)2-fluoro-2-deoxy-d-glucose: Validation of method. *Ann Neurol* 6:371-388.
- Phelps ME, Mazziotta JC, and Kuhl DE (1981) Metabolic mapping of the brain's response to visual stimulation: Studies in man. *Science* 211:1445-1448.
- Plum F, Gjedde A, and Samson FE (1976) Neuroanatomical functioning mapping by the radioactive 2-deoxy-D-glucose method. *Neurosci Res Program Bull* 14:457-518.
- Post RM, Kennedy C, Shinohara M, Squillace K, Miyaoka M, Suda S, Ingvar DH, and Sokoloff L (1979) Local cerebral glucose utilization in lidocaine-kindled seizures. *Neurosci Abstr* 5:196.
- Pulsinelli WA and Duffy TE (1979) Local cerebral glucose metabolism during controlled hypoxemia in rats. *Science* 204:626-629.
- Rakic P (1976) Prenatal genesis of connections subserving ocular dominance in the rhesus monkey. *Nature* 261:467-471.
- Reivich M, Jehle J, Sokoloff L, and Kety SS (1969) Measurement of regional cerebral blood flow with antipyrine-<sup>14</sup>C in awake cats. *J Appl Physiol* 27:296-300.
- Reivich M, Kuhl D, Wolf A, Greenberg J, Phelps M, Ido T, Cassella V, Fowler J, Hoffman E, Alavi A, Som P, and Sokoloff L (1979) The [<sup>18</sup>F]fluoro-deoxyglucose method for the measurement of local cerebral glucose utilization in man. *Circ Res* 44:127-137.
- Roth RH (1976) Striatal dopamine and gamma-hydroxybutyrate. *Pharmacol Ther* 2:71-88.
- Roth RH and Giarmann NJ (1966)  $\gamma$ -Butyrolactone and  $\gamma$ -hydroxybutyric acid. I. Distribution and metabolism. *Biochem Pharmacol* 15:1333-1348.
- Roy CS and Sherrington CS (1890) On the regulation of the blood supply of the brain. *J Physiol (London)* 11:85-108.
- Sacks W (1957) Cerebral metabolism of isotopic glucose in normal human subjects. *J Appl Physiol* 10:37-44.
- Sakurada O, Shinohara M, Klee WA, Kennedy C, and Sokoloff L (1976) Local cerebral glucose utilization following acute or chronic morphine administration and withdrawal. *Neurosci Abstr* 2:613.
- Sakurada O, Kennedy C, Jehle J, Brown JD, Carbin GL, and Sokoloff L (1978) Measurement of local cerebral blood flow with [<sup>14</sup>C]iodoantipyrine. *Am J Physiol* 234:H59-H66.

- Savaki HE, Kadekaro M, Jehle J, and Sokoloff L (1978)  $\alpha$ - and  $\beta$ -adrenoreceptor blockers have opposite effects on energy metabolism of the central auditory system. *Nature* 276:521–523.
- Scheinberg P and Stead EA Jr (1949) The cerebral blood flow in male subjects as measured by the nitrous oxide technique. Normal values for blood flow, oxygen utilization, and peripheral resistance, with observations on the effect of tilting and anxiety. *J Clin Invest* 28:1163–1171.
- Schwartz WJ (1978) A role for the dopaminergic nigrostriatal bundle in the pathogenesis of altered brain glucose consumption after lateral hypothalamic lesions. Evidence using the  $^{14}\text{C}$ -labeled deoxyglucose technique. *Brain Res* 158:129–147.
- Schwartz WJ and Gainer H (1977) Suprachiasmatic nucleus: Use of  $^{14}\text{C}$ -labeled deoxyglucose uptake as a functional marker. *Science* 197:1089–1091.
- Schwartz WJ, Sharp FR, Gunn RH, and Evarts EV (1976) Lesions of ascending dopaminergic pathways decrease fore-brain glucose uptake. *Nature* 261:155–157.
- Schwartz WJ, Davidsen LC, and Smith CB (1980) *In vivo* metabolic activity of a putative circadian oscillator, the rat suprachiasmatic nucleus. *J Comp Neurol* 189:157–167.
- Sejnowski TJ, Reingold SC, Kelley DB, and Gelperin A (1980) Localization of [ $^3\text{H}$ ]-2-deoxyglucose in single molluscan neurones. *Nature* 287:449–451.
- Sharp FR, Kauer JS, and Shepherd GM (1975) Local sites of activity-related glucose metabolism in rat olfactory bulb during olfactory stimulation. *Brain Res* 98:596–600.
- Shinohara M, Sakurada O, Jehle J, and Sokoloff L (1976) Effects of D-lysergic acid diethylamide on local cerebral glucose utilization in the rat. *Neurosci Abstr* 2:615.
- Shinohara M, Dollinger B, Brown G, Rapoport S, and Sokoloff L (1979) Cerebral glucose utilization: Local changes during and after recovery from spreading cortical depression. *Science* 203:188–190.
- Silverman MS, Hendrickson AE, and Clopton BM (1977) Mapping of the tonotopic organization of the auditory system by uptake of radioactive metabolites. *Neurosci Abstr* 3:11.
- Smith CB, Goochee C, Rapoport SI, and Sokoloff L (1980) Effects of ageing on local rates of cerebral glucose utilization in the rat. *Brain* 103:351–365.
- Sokoloff L (1960) Metabolism of the central nervous system *in vivo*. In: *Handbook of Physiology-Neurophysiology* (Field J, Magoun HW and Hall VE, eds), Vol. 3, Washington, DC, American Physiological Society, pp 1843–1864.
- Sokoloff L (1961) Local cerebral circulation at rest and during altered cerebral activity induced by anesthesia or visual stimulation. In: *The Regional Chemistry, Physiology and Pharmacology of the Nervous System* (Kety SS, and Elkes J, eds), Pergamon Press, Oxford pp 107–117.
- Sokoloff L (1966) Cerebral circulatory and metabolic changes associated with aging. *Res Publ Assoc Nerv Ment Dis* 41:237–254.
- Sokoloff L (1969) Cerebral circulation and behavior in man: Strategy and findings. In: *Psychochemical Research in Man* (Mandell AJ, and Mandell MP, eds), New York, Academic Press, pp 237–252.
- Sokoloff L (1976) Circulation and energy metabolism of the brain. In: *Basic Neurochemistry*, 2nd ed (Siegel GJ, Albers RW, Katzman R, and Agranoff BW, eds), Boston, Little, Brown, pp 388–413.
- Sokoloff L (1977) Relation between physiological function and energy metabolism in the central nervous system. *J Neurochem* 29:13–26.
- Sokoloff L (1978a) Local cerebral energy metabolism: Its relationships to local functional activity and blood flow. In: *Cerebral Vascular Smooth Muscle and Its Control*, Ciba Foundation Symposium 56 (Purves MJ and Elliott K, eds), Amsterdam, Elsevier/Excerpta Medica/North-Holland, pp 171–197.
- Sokoloff L (1978b) Mapping cerebral functional activity with radioactive deoxyglucose. *Trends Neurosci* 1(3):75–79.
- Sokoloff L (1979) The [ $^{14}\text{C}$ ]deoxyglucose method: Four years later. *Acta Neurol Scand (Suppl 70)* 60:640–649.
- Sokoloff L, Reivich M, Kennedy C, Des Rosiers MH, Patlak CS, Pettigrew KD, Sakurada O, and Shinohara M (1977) The [ $^{14}\text{C}$ ]deoxyglucose method for the measurement of local cerebral glucose utilization: Theory, procedure, and normal values in the conscious and anesthetized albino rat. *J Neurochem* 28:897–916.
- Sols A and Crane RK (1954) Substrate specificity of brain hexokinase. *J Biol Chem* 210:581–595.
- Webster WR, Serviere J, Batini C, and LaPlante S (1978) Autoradiographic demonstration with 2- [ $^{14}\text{C}$ ]deoxyglucose of frequency selectivity in the auditory system of cats under conditions of functional activity. *Neurosci Lett* 10:43–48.
- Wechsler LR, Savaki HE, and Sokoloff L (1979) Effects of *d*- and *l*-amphetamine on local cerebral glucose utilization in the conscious rat. *J Neurochem* 32:15–22.
- Wiesel TN, Hubel DH, and Lam DMK (1974) Autoradiographic demonstration of ocular dominance columns in the monkey striate cortex by means of transneuronal transport. *Brain Res* 79:273–279.
- Wolfson LI, Sakurada O, and Sokoloff L (1977) Effects of  $\gamma$ -butyrolactone on local cerebral glucose utilization in the rat. *J Neurochem* 29:777–783.
- Yarowsky PJ, Jehle J, Ingvar DH, and Sokoloff L (1979) Relationship between functional activity and glucose utilization in the rat superior cervical ganglion *in vivo*. *Neurosci Abstr* 5:421.
- Yarowsky P, Crane AM, and Sokoloff L (1980) Stimulation of neuronal glucose utilization by antidromic electrical stimulation in the superior cervical ganglion of the rat. *Neurosci Abstr* 6:340.